공학 석사 학위 논문

Gate Control of Mesoporous Silica Nanoparticle with α-Synuclein Coated Gold Nanoparticles and Its Application to Control of Cancer Metastasis

알파-시뉴클린 단백질로 코팅된 금 나노입자를 이용한 다공성실리카나노입자의 관문조절 그리고 암 전이 조절을 위한 응용

2016년 02월

서울대학교 대학원
화학생물공학부 전공
박 재 성

Gate Control of Mesoporous Silica Nanoparticle with α-Synuclein Coated Gold Nanoparticles and Its Application to Control of Cancer Metastasis

지도교수 백 승 렬

이 논문을 공학석사 학위논문으로 제출함

2016년 02월

서울대학교 대학원

화학생물공학부

박 재 성

박재성의 석사학위논문을 인준함

2016년 02월

위 원 장 김 병 기 (인)

부 위 원 장 백 승 렬 (인)

위 원 황 석 연 (인)

Abstract

Gate Control of Mesoporous Silica Nanoparitlcle with α-Synuclein Coated Gold Nanoparticles and Its Application to Control of Cancer Metastasis

Jaesung Park

School of Chemical and Biological Engineering

The Graduate School

Seoul National University

Over the last few decades, various kinds of drug delivery systems including liposome, nano-capsule, synthetic polymer, and etc have continuously been developed to maximize the therapeutic effect of drugs. However, developing the novel gate-keeping system with a controllable release mechanism for preventing the pre-mature release of cargo is the challenge remained. Herein, we report construction of protease responsive drug delivery system with secured gate keeping effect and propose its application in the control of cancer metastasis. The drug delivery system is mesoporous silica nanoparticle based with

its pores tightly capped by α-synuclein protein coated gold nanoparticles via the protein's unique adhesion property on silica surfaces. We have named it as the "Particles on a Particle" (PoP) system on account of its morphology that smaller particles are covering around a larger particle. In the *in vitro* cargo release test, using rhodamine6G dye as the model cargo, the PoP showed aorund 80% more effective gate keeping than bare system and the caps were stable at various pH ranges. Furthermore, selective cargo release was achieved by the digestion of α-synuclein by proteases such as trypsin, protease K and chymotrypsin. Protease inhibitor loaded PoP demonstrated its effectiveness in inhibiting the triggering protease indicating its usage in the treatment of the diseases where the level of certain protease is enhanced. As an expansion of this concept, the gate opening of PoP in the presence of matrix metalloproteinase, an endopeptidase known to facilitate the metastasis process of malignant tumor, was tested. Consequently, it was observed that PoP is responsive to matrix metalloproteinase and induced significant cargo release. These results emphasizes the potential of PoP as an enzyme responsive therapeutic nano-carrier which can prevent leaking of cargo and release drugs in response to the changes of patho-physicochemical microenvironment around the target disease.

Keywords: α-synuclein, Mesoporous Silica Nanoparticle, Drug Delivery System, Matrix Metalloproteinase, Protease Inhibition, Gate Control, Cancer Metastasis.

Student Number: 2013-23163

Contents

List of Tables

List of Figures

I. Introduction

1.1 Drug Delivery System

1.1.1 Gate Control

The field of drug delivery system is rapidly evolving as it provides promising potential for effective treatment of various diseases, including cancer. [1,2,3] In the realm of drug delivery system, the ideal vehicle must fulfill its mission of transporting sufficient amount of drugs to the target without leaking any guest molecule on its way. [4] In order to pursue this, it must have a specific gate control mechanism which can release guest molecule in a controlled manner. [5,6] Prevention of premature cargo release is important because it dwindles the side effects of drugs which is especially critical in tumor treatment where most of the antitumor drugs are toxic to cells. [8]

1.1.2 Mesoporous Silica Nanoparticle (MSN)

Many different types of drugs carriers have been developed in the past, for example, liposome, nanocapsule, polymer vesicle etc. [10, 19] Among those, mesoporous silica nanoparticle (MSN) is considered to be one of the most promising vehicle and continuously been studied to be applied in fields of biomedicine, catalysis, environmental protection, etc. [9,11]

As a nanocarrier, MSN possess many advantages like high surface area, ease of functionalization, high pore volume, stable mesoporous structure, and high biocompatibility. [10,12,13] Moreover, in our body, silica is converted to orthosilicic acid which can be

excreted through the kidneys. [4]

There are several types of MSNs such as MCM-41, MCM-48, and SBA-15 and each of them has different corresponding synthesis methods. [14,15] Among those, MCM-41 type is the most extensively researched one because of its simple, cost-effective, and controllable fabrication. [13] The synthesis of MCM-41 type was first reported by Mobil corportation in 1992. The step begins with utilizing cetyltrimethyl ammonium bromid (CTAB) for forming the soft template of the pores then silica particles are formed over it by the base-catalyzed sol-gel chemistry of tetraehtyl orthosilicate (TEOS). [14,16] (Figure 3)

1.1.3 Particles on a Particle (PoP)

In order to develop a drug delivery system that can achieve the goal of delivering the guest molecule to the desired target without leaking, we incorporated gold nanoparticles as the gatekeeper for blocking the pores of MSNs. Inspired from its morphology being, we have named this DDS as particles on a particle, PoP.

Previously, there have been studies which reported the use of nanoparticles such as cadmium sulfide and magnetite nanocrystals as the gatekeeper of MSNs and they showed precise control of the release of drug.[10,11,20] In many of these studies, the gatekeepers were chemically attached by a chemical linker, for example, disulfide linker. [10,12,17]. Nevertheless, we report the attachment of gold nanoparticles to MSN by the means of an adhesive protein called α-synuclein. Since there is no use of chemical linker in the fabrication of PoP, it is simple, facile and cost-effective method and higher biocompatibility is

expected for PoP.

1.2 α-Synuclein and α-Synuclein coated AuNP

1.2.1 α-Synuclein

The adhesive protein applied for PoP fabrication is α-synuclein. α-Synuclein is the major constituent protein of Lewy bodies, which is the defining hallmark of Parkinson's disease (PDs). [21-25] Although the pathologic mechanism of PDs is still unknown scientists believe that the misfolding of α-Synuclein is associated with the pathological process. [24-26]

α-Synuclein is expressed from SNCA gene and is constituted of 140 amino acids. [26] This protein is located in the synaptic vesicle of the dopaminergic neuron and the first isolation of α-Synuclein was done by Maroteaux et al. in 1988. [27] Interestingly, itt is soluble at its monomer state, however, under stimuli such as heat and shaking, it assembles into insoluble amyloid fibrils [24-27] The function of this cytosolic protein in physiology is still unrevealed but studies suggest that it can interacts directly with membranes. [26] Its unique characteristics of being able to self-assemble and interact with membranes make it a peculiar material candidate for various biomaterial applications.

1.2.1 α-Synuclein Coated Gold Nanoparticle (α–AuNP)

In our previous studies, we have reported the coating of gold nanoparticles with α-synuclein protein and its self-assembling characteristics followed by its subsequent applications in various fields from film assembly to SERS sensing. [28-31] (Figure 2) The coating

was conducted by covalent bond between the surface of gold nanoparticle and thiol group of α–synuclein mutant species, Y136C. Attachment of the C-term end of the protein on the surface of gold nanoparticles exposed the N-term ends of the protein on the outer surrounding. The reason behind this orientation is that N-term is suspected to be involved in the attachment to variable surfaces. The presence of protein coat on the particle was verified under TEM. (Figure 1) There are several particular features of α–AuNP which makes it highly applicable material for diverse purposes.

First, the protein on α–AuNP adhere on each other thus allowing the nanoparticles to self-assemble into regular infrastructures like pea-pod type chain and free-floating films. [30,31] Another unique feature of α–AuNP is its high adhesive tendency on silica surfaces. [29] (Figure 2) This adhesive characteristic is found to be strongest at the protein's isoelectric point, which is pH 4.4. [29] (Figure 2) SEM images revealed the high packing density of α–AuNPs on glass surface [29]. From this finding, the adhesive property is then adopted into making PoP DDS where α–AuNPs are adhered on silica surface of mesoporous silica nanoparticle for blocking the pores effectively.

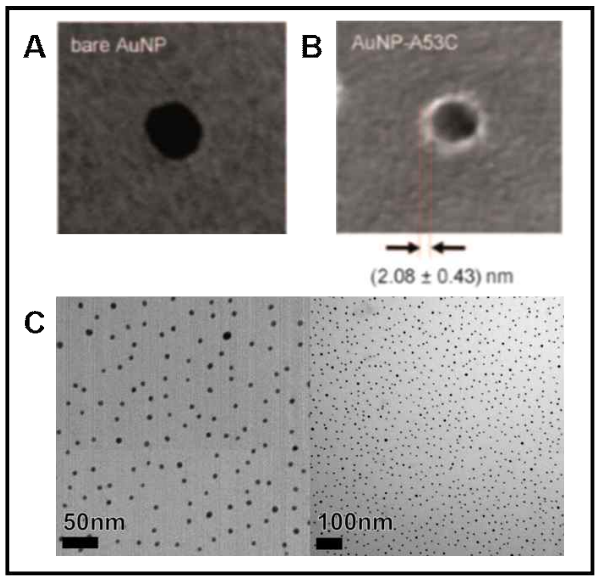

Figure 1. α-Synuclein coated AuNP (α-AuNP) TEM images of gold nanoparticles (A) Bare gold nanoparticle (B) α-synuclein protein coated gold nanoparticle, the protein layer surrounding the gold nanoparticle is visible after negative stain with 2% uranyl acetate. (C) α-AuNPs show high dispersity

Figure A and B: *Lee, D. et al. Angew. Chem. Int. Ed. 2011, 50, 1332-1337.

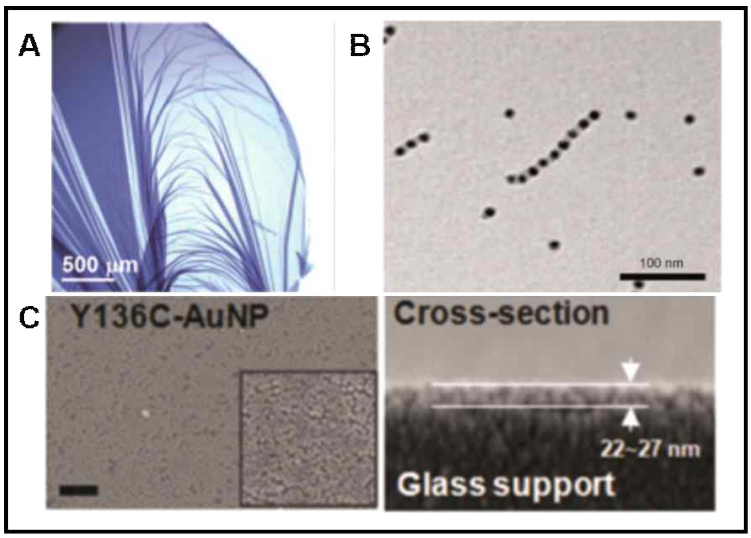

Figure 2. Infrastructure assemblies of α-AuNP (A) Optical image of α-AuNP free-standing film (B) TEM image of Pea-pod nano-chain assembly (C) Tight packing of α-AuNP on glass surface

Figure A: Lee, J. and Bhak G. et al. Angew. Chem. Int. Ed. 2015, 54, 4571-4576
Figure B: Lee, D. et al. Angew. Chem. Int. Ed. 2011, 50, 1332-1337
Figure C: Lee, D. et al. Langmuir 2011, 27, 12782-12787

1.3 Cancer Therapy by Drug Delivery System

1.3.1 Cancer Metastasis

Cancer is one of the deadliest disease to mankind causing enormous deaths globally every year. Significant development in the area of cancer therapy has been made for the past with improvement in diagnosis, surgical operation, and chemotherapy. [32] The conventional chemotherapy still has problems such as nonspecific distribution of drugs, excessive toxicity, and low targeting ability. [33] In order to overcome those obstacles, utilizing drug delivery system for cancer treatment has gathered interest of many scientists. [34] Therefore, an efficient drug delivery carrier with active targeting strategies would enhance the therapeutic efficacy in cancer treatment with minimizing toxic effect in normal cells. [33]

There are three major characteristics of cancer which are uncontrolled growth, mass formation and metastasis. [32] However, metastasis is considered to be the most fearsome and troublesome feature causing complexity to cancer therapy. [33,35] It is a process which tumor cells invade to surrounding tissues or into blood stream consequently forming metastases at other tissues. In cancer therapy, interfering cellular processes is an effective strategy thus inhibition of metastasis is thought to be a crucial target in cancer therapy. [36] Matrix metalloproteinase is known to be the potential target for therapeutics as the overexpession of this protien is associated with tumor invasion and metastasis. [36,37]

1.3.2 Matrix Metalloproteinase (MMP)

The matrix metalloproteinase are endopeptidase that belong to

the family of zinc-dependent proteinase. [36,37,38] They are involved in the degradation and remodelling of the extracelluar matrix. [36] More specifically, they consumes collagens as substrates and digest them. Subsequently, the digestion of extracelluar matrix facilitates tumor cells to be mobile and allow them to invade into blood vessels or lymph vessels. [37]

There are 18 members in the human MMP gene family which are structurely related and they are further categorized into five classes based on their structure and substrate specificity. [36] The five classes are collagenases, gelatinases, stromelysins, membrane type MMPs, and nonclassified MMPs. [36] Among them, type IV basement collagen digesting MMPs, MMP-2 and MMP-9, are the ideal drug targets because they are most consistently detected in tumor cells. [40]

Previous reports have indicated that there is a relationship between tumor metastasis and MMP overexpression. [40] Therefore, cancer researchers are actively designing and finding effective MMP inhibitors and developing drug delivery system that can successfully deliver MMP inhibitor to the cancer microenvironment. [36] When using DDS, a carrier must have a specific release mechanism that is responsive to selected stimuli. We believe the PoP system is expected to be responsive to the presence of MMPs as previous reports have proved reported that α-synuclein can be cleaved by MMPs. [37]

II. Materials and Methods

2.1 Materials

For the synthesis of mesoporous silica nanoparticles, tetraethylorthosilicate (TEOS) and hexadecyltrimethylammonium bromide (CTAB) were purchased from ACROS and sodium hydroxide (NaOH) and ethyl acetate (EtOAc) were purchased from Sigma Aldrich. Gold nanoparticles in 5nm size were purchased from Sigma Aldrich. 200-mesh carbon coated copper grids were purchased from Ted Pella Inc.. For the release profile, slide-A-Lyzer mini dialysis kit with 10,000 MWCO was purchased from ThermoFisher Scientific. Protease K was purchased from GenDEPOT and trypsin and chymotrypsin were purchased from Sigma Aldrich. Matrix Metalloproteinase-9 was purchased from AnaSpec. Nanopure water (18.1 MHz) was prepared from Direct-Q water purification system of Millipore. Other reagents used for protein purification were purchased from Sigma Aldrich.

2.2 Mesoporous Silica Nanoparticle Synthesis

50 mL of hexadecyltrimethylammonium bromide (CTAB) solution (0.1 g in 50 mL of nanopure water) was prepared and base (350 ul of 2M NaOH) was added. The mixture solution was heated to 75^{o}C and while gently stirring it 5 mL of tetraethylorthosilicate (TEOS) was added in dropwise manner. After 10 min, 0.5 mL of ethyl acetate (EtOAc) was added and the resulting mixture was vigorously stirred for 1 min and the sample was aged for 2.5 hour at the same temperature. After the aging, the solution turned to milky white and by

centrifugation white precipitate, MSN, was collected. The precipitate was resuspended in water and dispersed by water bath sonication. This washing step was performed twice with water and twice with ethanol. At last, to remove the CTAB from the pores of the synthesized MSN, 1.50 mL HCl was added to 150mL of MSN suspended ethanol solution then it was refluxed overnight.

2.3 Purification of α-Synuclein

Y136C α-synuclein DNA sequence was inserted into pRK172 plasmid. The resulting recombinant DNA was transformed in BL21 comeptent E.coli cell by heat-shock method. The cells were cultured on for 12 hours a LB agar plate containing 0.1 mg/ml ampicillin at 37^{o}C for screening. Then a colony is transferred into 100ml of LB media containing 0.1mg/ml ampicillin and incubated at 37^{o}C for 8 hours with shaking of 200rpm. After 8 hours, 1ml of the cultured solution was transferred into 1L of LB medium for the mass culture. The new media was incubated at same condition until the optical density at the wavelength of 600nm falls in the range between 0.6-0.8 then isopropano-b-D-thiogalactopyranoside (IPTG) was added for the induction of protein expression. Four hours later, the cells were harvested by centrifugation at 3600 rpm (Kontron) and the pellet was collected. The pellet was frozen and thawed first and resuspended in 200ml of lysis buffer containing (20mM tris/cl buffer, pH 7.5, 0.1M NaCl, 0.1mM PMSF, 1ug/ml Leupeptin, 2mM EDTA, 0.1mg/ml lysozyme and 10 units/ml of DNase). The cell lysate was centrifgued and surpernatant was collected and filtered through 0.22 um syringe filter. The protein crude extract was further purified by DEAE

Sephacyl anion exchange chromatography, S-200 Sephacryl Size exclusion chromatography and finally by S-sepharose cation exchange chromatograph. At each step, OD at 280nm was measured and noticeable peaks are verified by SDS-PAGE. After all three chromatograph steps, the protein solution was dialysed with 20mM MES buffer, pH 6.5, at 4^{o}C. The final protein solution was stored at −80^{o}C.

2.4 Preparation of the Protein Coated Gold Nanoparticles

50ul of 1mg/ml purified Y136C α-synuclein was mixed with 200ul of stock gold nanoparticle solution of 5nm. The resulting solution was incubated in a 4^{o}C refrigerator overnight. After incubation, the sample was centrifuged at 13200 rpm for 30minutes and discarded the supernatant. The pellet was washed with 200ul of MES buffer, pH 6.5, and the washing step was repeated twice more. The final pellet was collected and store in 4^{o}C.

2.5 Formation of Particles on a Particle (PoP)

Firstly, MSN was soaked in rhodamine6g dye solution to load the sample into the pores overnight. In a 1.5ml of transparent conical tube, 100ug of the MSN was reacted with 20 pmole of α-AuNP and the rest of the volume is filled with citrate buffer, pH 4.4, with the final volume of 100ul. The reaction has taken place for 2 hours then the PoP was collected by centrifugation at 9000rpm for 10min. The collected PoP was washed with 200ul of PBS buffer, pH 7.5, for 3 more times.

2.6 Characterization of MSN

The morphology and size of the synthesized MSN were observed on a transmission electron microscope(TEM) (JEM1010, JEOL, Jaoan) at 80 kV mode by loading sample on a carbon-coated copper grid. The particle size distribution was determined by a dynamic lgiht scattering (DLS) detector (Zetasizer Nano ZS, Malvern Co., UK). Using X-ray diffractometry (D8 Advance with Davinci, Bruker, Germany), low angle scan has been pursued to determine nanostructure of MSN. Nitrogen adsorption-desorption isotherms studies were carried by ASAP 2020 physisorption analyzer (USA). Before measurement the freeze dried MSN was degassed at 90^{o}C for 10 h to remove any contamination and moisture on the surface. Brunauer Emmett-Teller (BET) method was used to calculate the surface areas and the pore size distribution and pore volume were calculated by the Barrett-Joyner-Halenda (BJH) method.

2.7 UV/Vis Spectroscopy and FL Spectroscopy

Every UV/Vis measurement was conducted by UV/Vis spectrophotometer, Ultraspec 2100 Pro Amersham biosciences, USA. Also, all the fluorescence intensity of samples were measured by a fluorescence spectrometer, LS55, PelkinElmer, USA.

2.8 Cargo Release Assay

Cargo release from PoP was measured by placing slide-A-lyzer dialysis kit in a well plate. 200ul of PoP sample was pipetted into the dialysis kit and the well was filled with 1.5ml of PBS buffer and the solution in the well was measured for fluorescence intensity.

2.9 Enzyme Activity Assay

Hemoglobin substrate solution with concentration of 2.0% (w/v) was prepared by dissolving 0.2g of hemoglobin to 4ml of water. Then 800ul of 1M NaOH solution and 3.6g of urea was added to denature the hemoglobin. 50ul of 0.1units/ml enzyme solution was added to 250ul of the substrate solution. After selected time has passed, 500ul of TCA solution was added to precipitate down the undigested the proteins. The soluble peptide in the solution was collected by centrifugation and 150ul of F&C reagents were added to the solution. After letting the reaction to take place for 30 minutes, the absorbance of the solution was measured at 750nm.

III. Results and Discussions

3.1 Characterization of The Synthesized MSN

As illustrated on figure 3, the synthesis process of MCM-41 type of MSN was completed by using CTAB as the soft template for generating hexagonal pore array followed by sol-gel chemistry of the silica source, TEOS. In order to synthesize MSNs with uniform size of 100 nm and regular spherical morphology, the hydrolysis and the condensation reaction rates of the sol-gel chemistry was modulated. (Figure 3) The hydrolysis rate depends on the presence of NaOH, the base catalyst, and the condensation rate depends on the aging time hence establishing the optimal synthesis of MSN require modulation of these factors.

When the hydrolysis was uncontrolled and aging was proceeded afterward irregular shape of MSNs were synthesized. (Figure 4) Therefore, in order to control the hydrolysis rate, we have introduced ethyl acetate to scavenge the NaOH catalyst in the solution to dwindle the rate before proceeding to the condensation reaction. Furthermore, the aging time influenced the size of MSN, prolonging the aging time resulted in larger MSN, oppositely, shortening it resulted in smaller MSN. (Figure 4)

From these results, we have established the most optimal synthesis condition for regular spherical MSN with the size of 100 nm. The optimal condition involves letting the hydrolysis to take place to 10 minutes ethyl acetate was added then the aging was completed for 2.5 hours.

Under transmission electron microspocy (TEM), uniform size and shape of the resulting MSN was observed. (Figure 5) Also, dynamic light scattering was performed to further verify the size distribution of the MSN and it showed a narrow peak at 100 nm. (Figure 5) MCM-41 type of MSN has the defining hexagonal pore array nanostructure and to verify this Powder X-ray Diffraction (XRD) was conducted. The XRD pattern was measured at low angle from 0 to 10 and there are threes peaks indicating the miller indices of 100, 110, 200 hkl, which are the characteristic peaks observed from the hexagonal pore array structure. (Figure 5)

In addition, Brunauer-Emmett-Tell (BET) nitrogen gas adsorption-desoprtion isotherm analysis of powder form of the MSN was conducted to calculate the surface area as well as the Barrett-Joyner Halenda (BJH) analysis to calculate the pore size and

the volume. (Figure 6) The BET surface area was found to be 433.7221 g/m^2 and the BJH analysis verified pore size of 2.5 nm and pore volume of 0.79774 cm^3/g. (Table 1) Therefore, gold nanoparitcles with 5 nm in size are thought to be appropriate to block the pores with 2.5 nm in size and they are used in the PoP fabrication.

3.2 Confirmation of the fabricated PoP

As described earlier the particles-on-a-particle (PoP) drug delivery systems are fabricated by reacting α-AuNP and MSN at the isoelectric point of the protein, pH 4.4. (Figure 7) After the fabrication, TEM images of the PoP samples were taken and they show the α-AuNP are tightly clustered around MSN thus blocking the pores. (Figure 7). Even after several washing steps by centrifugation the PoP was stable thus indicating the considerably strong binding of the caps on the MSN. In other words, the PoP would be stable enough to endure the traveling through blood stream where it would experience shear pressure and colliding to other bio-molecules.

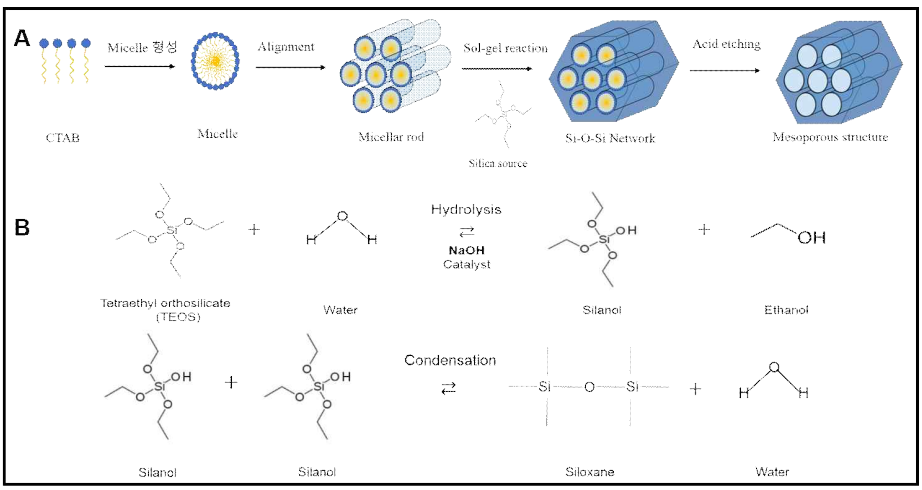

Figure 3. Synthesis of Mesoporous Silica Nanoparitcles (A) A Schematic illustration of MCM-41 type MSN synthesis process (B) Sol-gel Chemistry of tetraethylorthosilicate (TEOS)

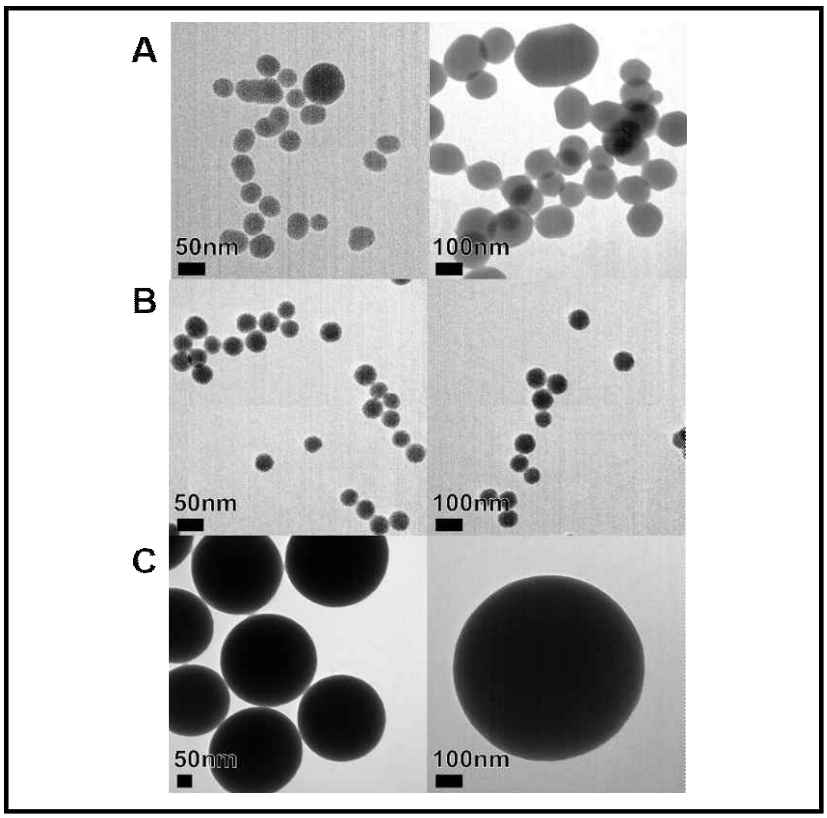

Figure 4. Size and morphology control of MSN TEM images of the synthesized MSN with different conditions (A) Without ethyl acetate treatment (B) Shortened aging time of 1 hour (C) Prolonged aging time of 4 hours.

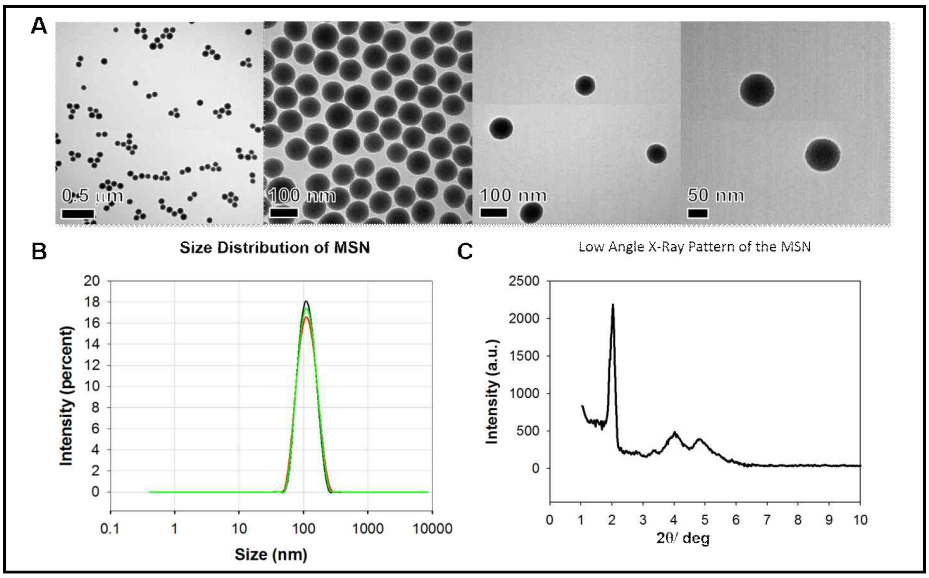

Figure 5. Analysis of the optimally synthesized MSN (A) TEM images of the spherical 100 nm MSN synthesized with the optimal condition (B) Dynamic Light Scattering (DLS) measurement showing narrow size distribution peak at 100 nm. (C) X-ray Diffraction (XRD) data showing three defining peaks of the hexagonal pore array at low angle.

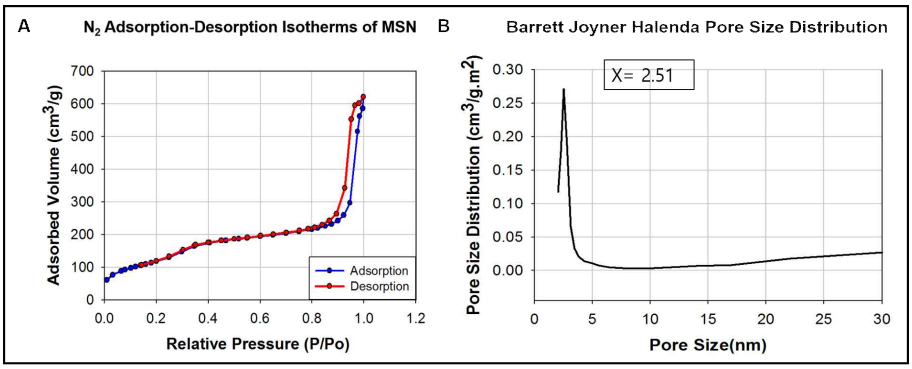

Figure 6. Brunauer-Emmett-Teller (BET) and Barrett-Joyner Halenda (BJH) Analysis (A) Nitrogen gas adsorption-desorption isotherm of the MSN (B) Graph of BJH pore size analysis

Diameter	BET Surface Area	Total Pore Volume	Pore Size	Zeta Potential
~100 nm	433.7221 (g/m^2)	0.79774 (cm^3/g)	2.5nm	-25.8

Table 1. Summary of the synthesized MSN characteristics

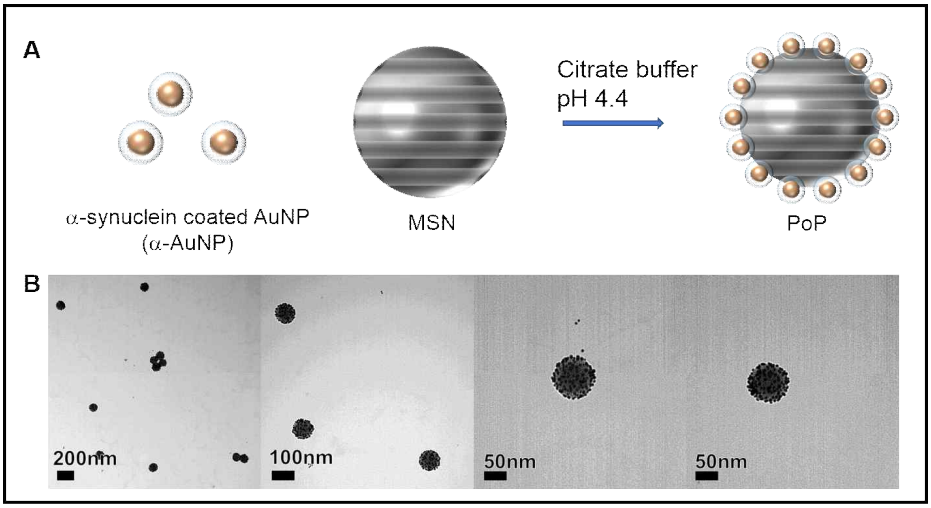

Figure 7. Fabrication of Particles-on-aParticle DDS (A) A Schematic illustration of PoP fabrication process (B) TEM images of PoP

3.3 Cargo Release Profile of Bare MSN vs. PoP

Cargo release profile was recorded using rhodamine6g (R6G) as the model cargo drug. The dye was loaded to MSN by suspending the MSN in R6G solution for overnight. Using a dialysis kit, the amount of R6G released to the solution was measured for bare MSN and PoP both loaded with the dye. Panel A in figure 8 is a graph which has been plotted by holding the florescence intensity measured for bare MSN sample at 300 minutes to be 100%. The graph shows a significant difference between the two samples, in comparison to bare MSN, PoP showed remarkably low cargo release. (Figure 8) More specifically, after 300 minutes, the R6G released from MSN was only 20% compared to that of MSN. Also, the TEM images of PoP after 300 minute demonstrate that the α-AuNPs were intactly blocking the pores. These results manifest the efficient gate keeping effect of PoP and its promising application as a drug carrier minimizing leaking of the loaded drug, in other words, preventing the side effects of the drug.

3.4 Effect of pH on The Cargo Release

Drug carriers travels through the physiological environment and experience various changes of the physico-chemical conditions, for example, the surrounding of tumor cells is acidic because they use glycolysis to botain extra energy. [34] For this reason, the effect of different pH on PoP was tested and likewise to the previous release profile cargo release was measured with R6G. In this test, PoP samples were placed in britton robinson buffers at different pH of 5, 6, 7, and 8. Within the measurement time of 300 minute, low cargo

release of around 20% was observed from all of the PoP samples at different pH. (Figure 9) Therefore, this indicates PoP drug delivery system is capable of enduring pH changes and maintaining efficient gate keeping.

3.5 Protease Induced Gate Opening of PoP

The cargo release results have manifested the effectiveness of the gate keeping capability of PoP. Since the α-AuNP caps are attached by the means of the adhesion characteristic of α-synuclein we expected presence of proteases would digest the protein consequently opening the gate. Therefore, the common proteases which are trypsin, protease K, and chymotrypsin were added to the R6G loaded PoP samples then the cargo release was measured.

It was observed that compared to the PoP without treatment, in all of the PoP samples treated with proteases, noticeably higher amount of R6G had been released during the time course of 30 minute. Also, the cargo release was highest in the PoP sample treated with trypsin and approximately 60 % was released after 300 minutes. This results also correlates to the abundance of lysin and arginine cleavage sites in the sequence of α-synuclein. TEM images of the samples treated with proteases after 300 minutes were taken to confirm the cap removal. (Figure 10) In all of the protease treated samples, the α-AuNPs were detached from MSN and found to be roaming in the solution.

These results indicate the gate opening of PoP can be achieved in the presence of PoP hence the system works in a controlled manner and it is enzyme responsive. Particularly, this suggests its potential application in protease activity control to protease sensors.

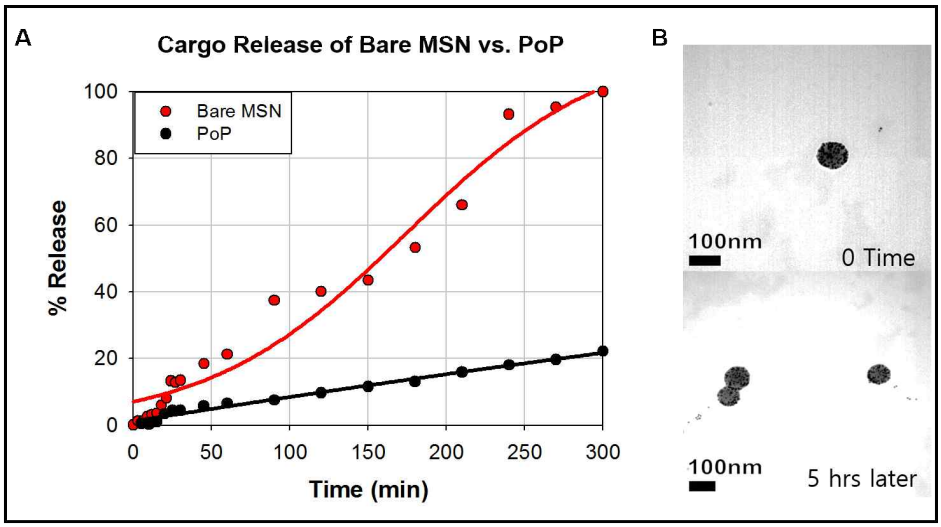

Figure 8. Cargo Release Profile of PoP vs. Bare MSN All samples were in PBS buffer of pH 7.5. Fluorescence intensity was measured to verify how much R6G has been released into the solution (A) Graph of the cargo releases of rhodamine6g (R6G) dye containing bare MSN and that of PoP. (B) TEM images of PoP at 0 time and 300 minutes later.

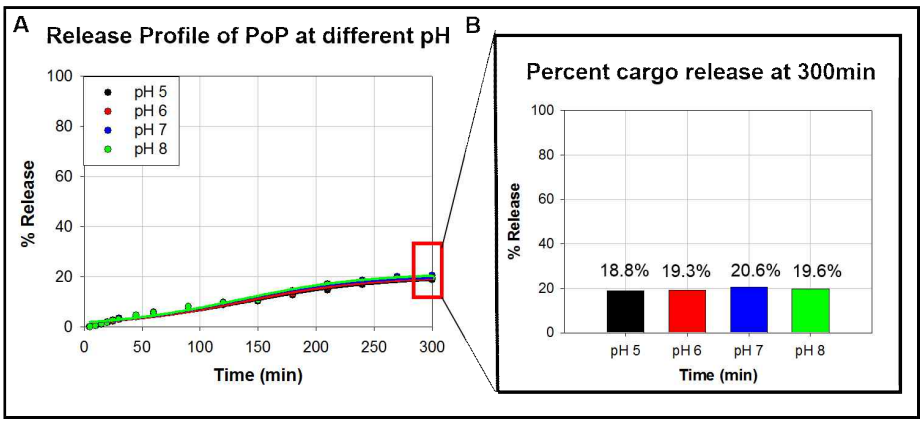

Figure 9. pH Effect on The Cargo Release of PoP R6G was used as the model cargo and Britton Robinson Buffer was used for pH control. (A) The Graph of percent cargo release of PoP samples at different pH for 300 minutes. (B) A bar graph of the amount released from each sample at 300 minute point.

3.6 Protease Activity Inhibition by PoP

The potential of PoP in the application of the inhibition of protease activity was verified with protease K using hemoglobin as substrate. In this test, the PoP samples were loaded with PMSF inhibitor and the digested substrate was quantified by measuring the amount of soluble peptide in the solution by reacting with Folin-Ciocalteu reagent.

The absorbance measurement graph shows highest digestion from the sample with protease only and lowest digestion from the samples with PMSF added as expected. (Figure 11) The PMSF loaded bare MSN also showed very low hemoglobin digestion and this is because the loaded PMSF are readily released since there is no gate control. The PMSF loaded PoP also manifested significant protease K inhibition effect, which means that the α-AuNP were detached from MSN by the digestion of protease K consequently the PMSF released from the pores successfully inhibited the protease K. Within the first 30 minutes, the digestion rate was higher for PoP compare to MSN due to the delay from the cap removal. After all, the results indicates the utiliity of PoP for inhibiting protease activity when loaded with inhibitors.

3.7 Matrix Metalloproteinase Induced Release

Finally, in order to show that PoP can be utilized for controlling the overexpression of MMP in the cancer metastasis process cargo release of PoP in the presence of MMP-9 was tested. Likewise to the previous assays R6G dye was used as model cargo and the fluorescence was measured for each sample treated with different MMP

concentrations. PoP without any proteases and PoP with trypsin treatment were set as the controls. In the presence of MMP, high fluoresence intensity compared to the control was observed and it seemed to correlate to the concentration of MMP treated. (Figure 12) Especially the sample with 30 ng/ul MMP-9 treatment showed noticeably high R6G release similar to the trypsin sample. Therefore, it is clear that the MMP-9 cleaved α-synuclein of the α-AuNP thus induced pore opening. Therefore, we can expect a promising application of PoP in MMP activity control, more specifically, a therapeutic strategy for cancer metastasis.

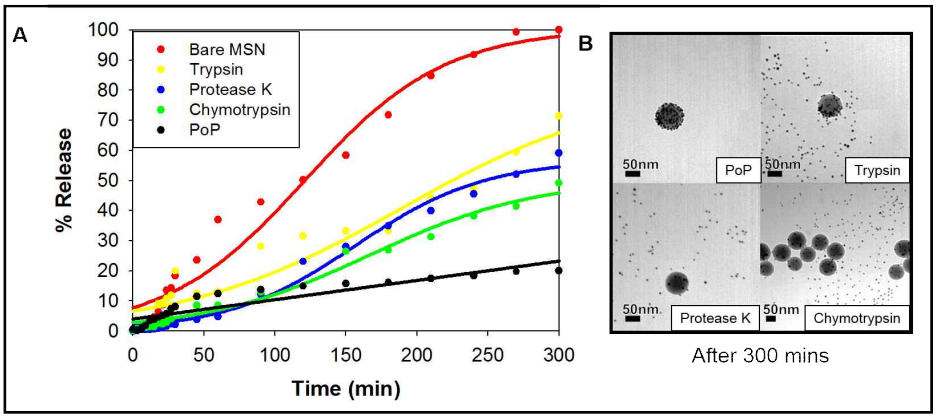

Figure 10. Proteases Induced Cargo Release of PoP The cargo release of PoP using R6G as the model drug was measured in the presence of different proteases. All protease concentrations were 30 ug/ul (A) A graph of R6G rhodamine release profile with samples incubated with the designated proteases. (B) TEM images of samples of PoP, trypsin treated PoP, protease K treated PoP, and chymotrypsin treated PoP after 300 minutes.

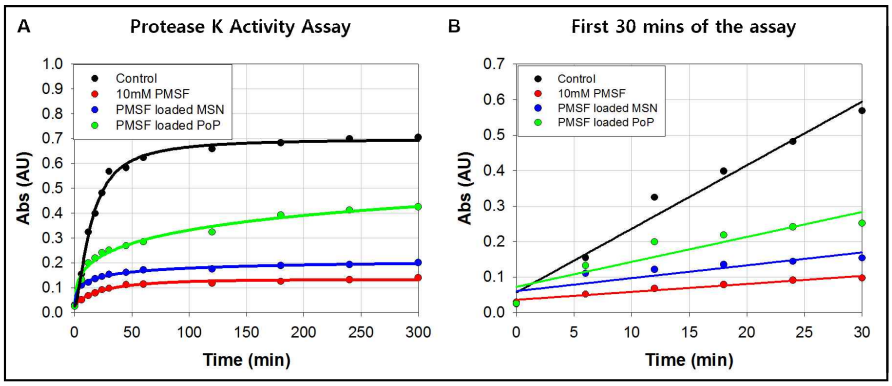

Figure 11. Protease K Activity Assay Urea denatured hemglobin was used as substrate for the assay. The soluble peptide digested by protease K was quantified by measuring the absorbance after reacting with Folin-Ciocalteu reagent (A) A graph showing change in protease K activity of samples of control (no treatment), 10mM PMSF, PMSF loaded MSN, and PMSF loaded PoP. (B) The first 30 minutes of the graph on the left.

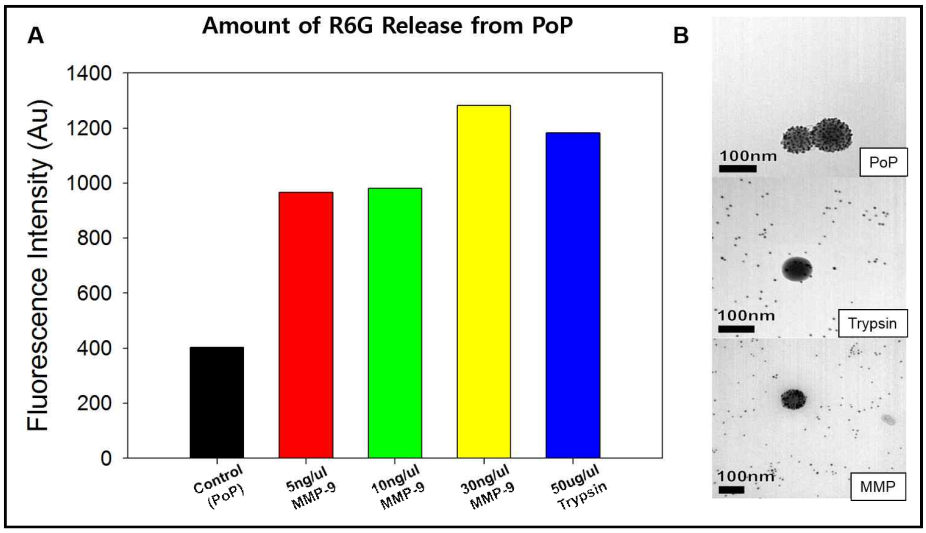

Figure 12. MMP Induced Cargo Release from PoP Rhodamine6G dye was used as the model cargo and the fluorescence of the supernatant was measured after incubation with the assigned protease type and concentration at 37 for 1 hour. (A) A bar graph of the fluorescence intensity measured for each sample. (B) TEM images of the PoP samples after incubation.

IV. Conclusions

In this research, we have introduced particles-on-a-particle carrier model which is a novel drug delivery system with remarkable gate keeping effect and controllable cargo release mechanism. We began with demonstrating the fabrication process of PoP including synthesis of mesoporous silica nanoparticle followed by assays for cargo release profile of PoP, cargo release from PoP by protease digestion, usage of PoP for inhibiting protease activity, and finally MMP responsive cargo release.

First of all, in the MSN synthesis part, we were able to synthesize uniform 100 nm MSNs with spherical shape by modulating the hydrolysis rate and the condensation rate of sol-gel chemistry of silica. The resulting MSNs were analyzed by TEM, DLS, XRD, and BET/BJH for determining the size distribution, morphology, surface area, nano-structure, and pore size and volume. Table 1 shows the summary of the characteristics of the synthesized MSN. After obtaining MSNs, they were incubated with α-AuNP in citrate buffer of pH 4.4 and the intact PoP fabricated and were verified by TEM analysis.

Next, the cargo release profile of R6G model cargo revealed the secured gate keeping effect as well as its stability at various pH ranges. In addition, PoP demonstrated that the controlled cargo release was achieved by the digestion of proteases meaning that PoP system could be utilized for applications like protease sensor for conditions where change in level of certain proteases is important. Then utilizing PoP for inhibiting protease K activity was carried out and PoP

effectively inhibited the protease indicating that same consequence can be expected for controlling MMP activity.

Finally, a successful cargo release of the R6G containing PoP was observed in the presence of MMP-9 indicaitng that PoP is MMP responsive. Therefore, it is likely that PoP DDS can be applied for the MMP activity control which is the crucial target in cancer metastasis process. This means that PoP has a promising potential as a drug delivery carrier for the treatment of diseases where controlling certain type of protease is the key factor.

V. References

[1]. JunSeok, Lee, Juhee Park, Kaushik Singha and Won Jong Kim (2012) Mesoporous silica nanoparticle facilitated drug release through cascade photosensitizer activation and cleavage of singlet oxygen sensitive linker. *ChemComm*, 49, 1545-1547.

[2]. Igor I., Slwoing, Brian G. Trewyn, Supratim Giri, and Victor S.Y. Lin (2007) Mesoporous Silica Nanoparticles for Drug Delivery and Biosensing Applications. *Adv. Funct. Mater.*, 2007, 17, 1225-1236.

[3]. Zongxi Li, Jonathan C. Barnes, Aleksandr Bosoy, J. Fraser Stoddart and Jeffrey I. Zink (2012) Mesoporous silica nanoparticles in biomedical applications. *Chem. Soc. Rev*., 2012, 41, 2590-2605

[4]. Xin Chen, Xiaoyu Cheng, Alexander H. Soeriyadi, Sharon M. Sagnella, Xun Lu, Jason A. Scott, Stuart B. Lowe, Maria Kavallaris, and J. Justin Gooding (2014) Stimuli-responsive functionalized mesoporous silica nanoparticles for drug release in response to various biological stimuli. *Biomater. Sci*., 2, 121-130

[5] Fangqiong Tang, Linlin Li, and Dong Chen (2012) Mesoporous Silica Nanoparticles: Synthesis, Biocompatibility and Drug Delivery. *Adv. Mater,* 2012, 24, 1504-1534

[6] Qianjun He and Jianlin Shi (2011) Mesoporous silica nanoparticle based nano drug delivery systems: synthesis, controlled drug release and delivery, pharmacokinetics and biocompatibility. *J. Mater. Chem.*, 2011, 21, 5845-5855

[7] Kevin C.-W. Wu and Yusuke Yamauchi (2012) Controlling physical features of mesoporous silica nanoparticles (MSNs) for emerging applications. *J. Mater. Chem.*, 2012, 22, 1251-1256

[8] Supratim Giri, Brian G. Trewyn, Michael P. Stellmaker, and Victor S.-Y. Lin (2005) Stimuli-Responsive Controlled-Release Delivery System Based on Mesoporous Silica Nanorods Capped with Magnetic Nanopaticles. *Angew. Chem. Int. Ed.* 2005, 44, 5038-5044

[9] Buckley, A.M. and Greenblatt, M.J. (1994) Sol-Gel Preparation of Silica Gels.

Chem. Ed. 1994, 71(7), 599

[10] Igor I. Slowing, Juan L. Vivero-Escoto, Chia-Wen Wu, and Victor S.-Y. Lin (2008) Mesoporous Silica Nanoparticle as controlled release drug delivery and gene transfection carriers. *Advanced Drug Delivery Reviews*, 2008, 60, 1278-1288

[11] Ji Eun Lee, Nohyun Lee, Hyoungsu Kim, Jaeyun Kim, Seung Hong Choi, Jeong Hyun Kim, Taeho Kim, In Chan Song, Seung Pyo Park, Woo Kyung Moon, and Taeghwan Hyeon (2010) Uniform Mesoporous Dye-Doped Silica Nanoparticles Decorated with Multiple Magnetite Nanocrystals for Simultaneous Enhanced Magnetic Resonance Imaging, Fluorescence Imaging, and Drug Delivery. *J. Am. Chem. Soc.* 2010, 132, 552-557

[12] Qianjun He and Jialin Shi (2014) MSN Anti-Cancer Nanomedicines: Chemotherapy Enhancement, Overcoming of Drug Resistance, and Metastasis Inhibition. *Adv. Mater.* 2014, 26, 391-411

[13] Igor Slowing, Brian G. Trewyn, and VIctor S.-Y. Lin (2006) Effect of Surface Functionalization of MCM-41 Type Mesoporous Silica Nanoparticles on the Endocytosis by Human Cancer Cells. *J. AM. Chem. Soc.* 2006, 128, 14792-14793

[14] Jessica M. Rosenholm, Cecilia Sahlgren and Mika Linden (2010) Towards multifunctional, targeted drug delivery systems using mesoporous silica nanoparticles − opportunities & challenges. *Nanoscale,* 2010, 2, 1870-1883

[15] Yanna Cui, Haiqing Dong, Xiaojun Cai, Deping Wang, and Yongyong Li (2012) Mesoporous Silica Nanoparticles Capped with Disulfide-Linked PEG Gatekeepers for Glutathione-Mediated Controlled Release. *Appl. Mater. Interfaces* 2012, 4, 3177-3183

[16] Amirali Popat, Sandy Budi Hartono, Frances Stahr, Jian Liu, Shi Zhang Qiao and Gao Qing (Max) Lu (2011) Mesoporous Silica Nanoaprticle for bioadsorption, enzyme immobilisation, and delivery carriers. *Nanoscale,* 2011, 3, 2801

[17] Juan L. Vivero-Escoto, Igor I. Slowing, Chian-Wen Wu, and Victor S.-Y. Lin (2009) Photoinduced intracellular Controlled Release Drug Delivery in Human Cells by Gold-Capped Mesoporous Silica Nanosphere. J. Am. Chem. Soc. 2009, 131, 3462-3463

[18] Piaoping Yang, Shili Gai, and Jun Lin (2012) Functionalized mesoporous silica materials for controlled drug delivery. *Chem. Soc. Rev.,* 2012, 41, 3679-3698

[19] Kristina Riehemann, Stefan W. Schneider, Thomas A. Luger, Biana Godin, Mauro Ferrari, and Harald Fuchs (2009) Nanomedicine-Challenge and Perspectives.

Angew. Chem. Int. Ed., 2009, 48, 872-897

[20] Cheng-Yu Lai, Brian G. Trewyn, Dusan M. Jeftinija, Ksenija Jeftinija, Shu Xu, Srdija Jeftinija, and Victor S.-Y. Lin (2003) A Mesoporous Silica Nanosphere-Based Carrier System with Chemically Removable CdS Nanoparticle Caps for Stimuli-Responsive Controlled Release of Neurotransmitters and Drug Molecules. *J. Am. Chem. Soc.*, 2003, 125, 4451-4459.

[21] Maria Grazia Spillantini, Marie Luise Schmidt, Virginia M.-Y. Lee, John Q. Trojanowski,, Ross Jakes, and Michel Goedert (1997) α-synuclein in Lewy Bodies., Nature, 1997, vol 388, 28

[22] Minami Baba, Shiegeo Nakajo, Pang-Hsien Tu, Taisuke Tomita, Kazuyasu Nakaya, Virginia M.-Y. Lee, John Q. Trojanowski, and Takeshi Iwatsubo (1998) Aggregation of α-synuclein in Lewy Bodies of Sporadic Parkinson's Disease and Dementia with Lewy Bodies, *American Journal of Pathology,* Vol 152, No 4, April 1998

[23] C. B. Lucking and A. Brice (2000) Alpha-synuclein and Parkinson's disease. CMLS, *Cell. Mol. Life Sci.* 57 (2000) 1894-1908

[24] P.M. Mattila, J. O. Rinne, H. Helenius, D. W. Dickson, and M. Roytta (2000) Alpha-synuclein-immunoreactive cortical Lewy bodies are associated with cognitive impairment in Parkinson's disease. *Acta Neuropathol* (2000) 100: 285-290

[25] Benoit I. Giasson, Mark S. Forman, Makoto Higuchi, Lawrence I. Golbe, Charles L. Graves, Paul T. Kotzbauer, John Q. Trojanowski, Virginia M.-Y. Lee (2003) Initiation and Synergistic Fibrillization of Tau and Alpha-Synuclein. *Science* 300, 636 (2003)

[26] Tiago Fleming Outeiro and Susan Lindquist (2003) Yeast Cells Provide Insight into Alpha-Synuclein Biology and Pathobiology., *Science* 302, 1772 (2003)

[27] Pavan K. Auluck, Gabriela Caraveo, and Susan Lindquist (2010), α-synuclein: Membrane Interactions and Toxicity in Parkinson's Disease., Annu. Rev. Cell Dev. Biol. 2010. 26:211-33

[28] Daekyun Lee, Young-Jun Choe, Minwoo Lee, Dae H. Jeong, and Seung R. Paik (2011) Protein-Baesd SERS Technology Monitoring the Chemical Reactivity on an α-synuclein-medicated Two-Dimensional Array of Gold Nanoparticles., Langmuir 2011, 27, 12782-12787

[29] Daekyun Lee, Je Won Hong, Chanyoung Park, Hagyeol Lee, Ji Eun Lee,

Taeghwan Hyeon, and Seung R. Paik (2014) $Ca2^{+}$-Dependent Intracellular Drug Delivery System Developed with "Raspberry-Type" Particles-on-a-Particle Comprising Mesoporous Silica Core and α-Synuclein-Coated Gold Nanoparticles., *Acs Nano,* 2014, Vol 8, No. 9, 8887-8895

[30] Daekyun Lee, Young-Jun Choe, Yeon Sun Choi, Ghibom Bhak, Jihwa Lee, and Seung R. Paik (2011) Photoconductive of Pea-Pod-Type Chains of Gold Nanoparticles Encapsulated within Dielectric Amyloid Protein Nanofibrils of α-Synuclein. *Angew. Chem. Int. Ed.,* 2011, 50, 1132-1337

[31] Junghee Lee, Ghibom Bhak, Ji-Hye Lee, Woohyun Park, Minwoo Lee, Daekyun Lee, Noo Li Jeon, Dae H. Jeong, Kookheon Char, and Seung R. Paik (2015) Free Standing Gold-Nanoparticle Monolayer Film Fabricated by Protein Self-Asembly of α-Synuclein., *Angew. Chem. Int. Ed.,* 2015, 54, 4571-4576.

[32] Isaiah J. Fidler (2003) The pathogenesis of cancer metastasis: the 'seed and soil' hypothesis revisited, *Nature Reviews*, volume 3, 1-6

[33] Wadih Arap, Renata Pasqualini, and Erkki Ruoslahti (1998) Cancer Treatment by Targeted Drug Delivery to Tumor Vasculature in a Mouse Model, *Science*, 279, 377

[34] Kwangjae Cho, Xu Wang, Shuming Nie, Zhuo (Georgia) Chen, and Dong M. Shin (2008) Therapeutic Nanoparticles for Drug Delivery in Cancer, *Clin. Cancer Res*., 2008; 14:1310-1316

[35] John F. R. Kerr, Clay M. Winterford, Assoc. Dipl. Appl. Biol., and Brian V. Haromon (1994) Apoptosis, *Cancer*, 1994, Volume 73, No. 8

[36] Manuel Hidalgo, S. Gail Eckhardt (2001) Development of Matrix Metalloproteinase Inhibitors in Cancer Therapy, *Journal of the National Cancer Institute*, Vol.93, No. 3

[37] Johannes Levin, Armin Giese, Kai Boetzel, Lars Israel, Tobias Hogen, Georg Nubling, Hans Kretzschmar, and Stefan Lorenzl (2008) Increased α-synuclein aggregation following limited cleavage by certain matrix metalloproteinases, *Experimental Neurology*, 215, 201-208

[38] M.W. Roomi, J.C. Monterrey, T. Kalinovsky, M. Rath and A. Niedzwiecki (2009) Patterns of MMP-2 and MMP-9 expression in human cancer cell lines, *Oncology Reports,* 21: 1323-1333

[39] Gabriele Bergers, Rolf Brekken, Gerald McMahon, Thiennu H. Vu, Takeshi Itoh, Kazuhiko Tamaki, Kazuhiko Tanzawa, Philip Thorpe, Shigeyoshi Itohara, Zena Werb,

and Douglas Hanahan (2000) Matrix Metalloproteinase-9 triggers the angiogenic switch during carcinogenesis, *Nature Cell Biology,* Vol 2

[40] Stanley Zucker and Jian Cao (2009) Selective Matrix metalloproteinase (MMP) inhibitors in cancer therapy: ready for prime time?, *Cancer Biol Ther.* 2009; 8(24): 2371-2373

국문 초록

최근 몇 년 동안 라이포좀, 나노캡슐, 합성 폴리머 등과 같은 다양한 약물전달 시스템들이 약물의 치료효과를 극대화하기 위한 목적으로 지속적으로 개발되어 왔다. 그러나 선택적 약물 방출이 가능한 새로운 게이트 방지 시스템 기작을 개발하는 것은 아직까지 풀어야할 숙제이다. 본 연구에서는 프로테아제의 반응하며 효과적인 게이트 방지 능력를 지닌 약물전달 시스템의 제작과 암 전이 조절을 위한 응용으로서의 가능성을 제시한다.

본 약물전달 시스템은 다공성의 실리카 나노입자를 기반으로 하며 α-synuclein 단백질의 특이적인 흡착 성질을 이용하여 이 단백질로 코팅되어진 금나노입자로 다공을 막는다. 우리는 많은 금나노입자들이 하나의 실리카 나노입자를 감싸고 있는 모양을 바탕으로 이 약물전달 시스템을 Particles-on-a-Particle (PoP)으로 명명하였다.

Rhodamine6G 형광물질을 이용한 in vitro 약물방출 연구를 통해 PoP의 확실한 게이트 관리 효과를 증명하였으며 다양한 pH 조건에서도 안정함을 확인하였고 이는 곧 약물이 무작위로 방출되는 것을 방지할 수 있음을 의미한다. 더 나아가 선택적인 약물방출이 trypsin, protease K 그리고 chymotrypsin과 같은 프로테아제로 인해 가능한 것을 확인하였다. 또한 프로테아제의 억제제를 탑재한 PoP을 이용하여 프로테아제에 의한 억제제가 방출과 이로 인한 해당 프로테아제의 억제가 가능하다는 것을 확인하였다.

마지막으로 암전이 과정에서 extracelluar matrix를 분해시키는 중요한 타겟으로 여겨지는 Matrix metalloproteinase의 과발현 조절을 위한 활용을 목적으로 MMP에 의한 PoP에 약물방출을 확인하였다. 이를 통해 상당한 양의 탑재된 약물이 MMP에 의해 방출이 되는

것을 관찰하였으며 이러한 결과들은 효소 반응적인 치료용 나노캐리어로서의 PoP의 가능성을 강조한다. 그리고 이는 곧 약물의 조절되지 못한 소실의 방지를 의미한다. 마지막으로 PoP이 생체내에 병리적 물리화학적 변화에 반응하는 효과적인 약물전달체가 될 수 있을 것이라 기대된다.

주요 단어: **α-synuclein, Mesoporous Silica Nanoparticle, Drug Delivery System, Matrix Metalloproteinase, Protease Inhibition, Gate Control, Cancer Metastasis.**

학번: 2013-23163

공학 석사 학위 논문

Gate Control of Mesoporous Silica Nanoparticle with α-Synuclein Coated Gold Nanoparticles and Its Application to Control of Cancer Metastasis

알파-시뉴클린 단백질로 코팅된 금 나노입자를 이용한 다공성실리카나노입자의 관문조절 그리고 암 전이 조절을 위한 응용

2016년 02월

서울대학교 대학원
화학생물공학부 전공
박 재 성

Gate Control of Mesoporous Silica Nanoparticle with α-Synuclein Coated Gold Nanoparticles and Its Application to Control of Cancer Metastasis

지도교수 백 승 렬

이 논문을 공학석사 학위논문으로 제출함

2016년 02월

서울대학교 대학원

화학생물공학부

박 재 성

박재성의 석사학위논문을 인준함

2016년 02월

위 원 장 김 병 기 (인)

부 위 원 장 백 승 렬 (인)

위 원 황 석 연 (인)

Abstract

Gate Control of Mesoporous Silica Nanoparitlcle with α-Synuclein Coated Gold Nanoparticles and Its Application to Control of Cancer Metastasis

Jaesung Park

School of Chemical and Biological Engineering

The Graduate School

Seoul National University

Over the last few decades, various kinds of drug delivery systems including liposome, nano-capsule, synthetic polymer, and etc have continuously been developed to maximize the therapeutic effect of drugs. However, developing the novel gate-keeping system with a controllable release mechanism for preventing the pre-mature release of cargo is the challenge remained. Herein, we report construction of protease responsive drug delivery system with secured gate keeping effect and propose its application in the control of cancer metastasis. The drug delivery system is mesoporous silica nanoparticle based with

its pores tightly capped by α-synuclein protein coated gold nanoparticles via the protein's unique adhesion property on silica surfaces. We have named it as the "Particles on a Particle" (PoP) system on account of its morphology that smaller particles are covering around a larger particle. In the *in vitro* cargo release test, using rhodamine6G dye as the model cargo, the PoP showed aorund 80% more effective gate keeping than bare system and the caps were stable at various pH ranges. Furthermore, selective cargo release was achieved by the digestion of α-synuclein by proteases such as trypsin, protease K and chymotrypsin. Protease inhibitor loaded PoP demonstrated its effectiveness in inhibiting the triggering protease indicating its usage in the treatment of the diseases where the level of certain protease is enhanced. As an expansion of this concept, the gate opening of PoP in the presence of matrix metalloproteinase, an endopeptidase known to facilitate the metastasis process of malignant tumor, was tested. Consequently, it was observed that PoP is responsive to matrix metalloproteinase and induced significant cargo release. These results emphasizes the potential of PoP as an enzyme responsive therapeutic nano-carrier which can prevent leaking of cargo and release drugs in response to the changes of patho-physicochemical microenvironment around the target disease.

Keywords: α-synuclein, Mesoporous Silica Nanoparticle, Drug Delivery System, Matrix Metalloproteinase, Protease Inhibition, Gate Control, Cancer Metastasis.

Student Number: 2013-23163

Contents

List of Tables

List of Figures

I. Introduction

1.1 Drug Delivery System

1.1.1 Gate Control

The field of drug delivery system is rapidly evolving as it provides promising potential for effective treatment of various diseases, including cancer. [1,2,3] In the realm of drug delivery system, the ideal vehicle must fulfill its mission of transporting sufficient amount of drugs to the target without leaking any guest molecule on its way. [4] In order to pursue this, it must have a specific gate control mechanism which can release guest molecule in a controlled manner. [5,6] Prevention of premature cargo release is important because it dwindles the side effects of drugs which is especially critical in tumor treatment where most of the antitumor drugs are toxic to cells. [8]

1.1.2 Mesoporous Silica Nanoparticle (MSN)

Many different types of drugs carriers have been developed in the past, for example, liposome, nanocapsule, polymer vesicle etc. [10, 19] Among those, mesoporous silica nanoparticle (MSN) is considered to be one of the most promising vehicle and continuously been studied to be applied in fields of biomedicine, catalysis, environmental protection, etc. [9,11]

As a nanocarrier, MSN possess many advantages like high surface area, ease of functionalization, high pore volume, stable mesoporous structure, and high biocompatibility. [10,12,13] Moreover, in our body, silica is converted to orthosilicic acid which can be

excreted through the kidneys. [4]

There are several types of MSNs such as MCM-41, MCM-48, and SBA-15 and each of them has different corresponding synthesis methods. [14,15] Among those, MCM-41 type is the most extensively researched one because of its simple, cost-effective, and controllable fabrication. [13] The synthesis of MCM-41 type was first reported by Mobil corportation in 1992. The step begins with utilizing cetyltrimethyl ammonium bromid (CTAB) for forming the soft template of the pores then silica particles are formed over it by the base-catalyzed sol-gel chemistry of tetraehtyl orthosilicate (TEOS). [14,16] (Figure 3)

1.1.3 Particles on a Particle (PoP)

In order to develop a drug delivery system that can achieve the goal of delivering the guest molecule to the desired target without leaking, we incorporated gold nanoparticles as the gatekeeper for blocking the pores of MSNs. Inspired from its morphology being, we have named this DDS as particles on a particle, PoP.

Previously, there have been studies which reported the use of nanoparticles such as cadmium sulfide and magnetite nanocrystals as the gatekeeper of MSNs and they showed precise control of the release of drug.[10,11,20] In many of these studies, the gatekeepers were chemically attached by a chemical linker, for example, disulfide linker. [10,12,17]. Nevertheless, we report the attachment of gold nanoparticles to MSN by the means of an adhesive protein called α-synuclein. Since there is no use of chemical linker in the fabrication of PoP, it is simple, facile and cost-effective method and higher biocompatibility is

expected for PoP.

1.2 α-Synuclein and α-Synuclein coated AuNP

1.2.1 α-Synuclein

The adhesive protein applied for PoP fabrication is α-synuclein. α-Synuclein is the major constituent protein of Lewy bodies, which is the defining hallmark of Parkinson's disease (PDs). [21-25] Although the pathologic mechanism of PDs is still unknown scientists believe that the misfolding of α-Synuclein is associated with the pathological process. [24-26]

α-Synuclein is expressed from SNCA gene and is constituted of 140 amino acids. [26] This protein is located in the synaptic vesicle of the dopaminergic neuron and the first isolation of α-Synuclein was done by Maroteaux et al. in 1988. [27] Interestingly, itt is soluble at its monomer state, however, under stimuli such as heat and shaking, it assembles into insoluble amyloid fibrils [24-27] The function of this cytosolic protein in physiology is still unrevealed but studies suggest that it can interacts directly with membranes. [26] Its unique characteristics of being able to self-assemble and interact with membranes make it a peculiar material candidate for various biomaterial applications.

1.2.1 α-Synuclein Coated Gold Nanoparticle (α–AuNP)

In our previous studies, we have reported the coating of gold nanoparticles with α-synuclein protein and its self-assembling characteristics followed by its subsequent applications in various fields from film assembly to SERS sensing. [28-31] (Figure 2) The coating

was conducted by covalent bond between the surface of gold nanoparticle and thiol group of α–synuclein mutant species, Y136C. Attachment of the C-term end of the protein on the surface of gold nanoparticles exposed the N-term ends of the protein on the outer surrounding. The reason behind this orientation is that N-term is suspected to be involved in the attachment to variable surfaces. The presence of protein coat on the particle was verified under TEM. (Figure 1) There are several particular features of α–AuNP which makes it highly applicable material for diverse purposes.

First, the protein on α–AuNP adhere on each other thus allowing the nanoparticles to self-assemble into regular infrastructures like pea-pod type chain and free-floating films. [30,31] Another unique feature of α–AuNP is its high adhesive tendency on silica surfaces. [29] (Figure 2) This adhesive characteristic is found to be strongest at the protein's isoelectric point, which is pH 4.4. [29] (Figure 2) SEM images revealed the high packing density of α–AuNPs on glass surface [29]. From this finding, the adhesive property is then adopted into making PoP DDS where α–AuNPs are adhered on silica surface of mesoporous silica nanoparticle for blocking the pores effectively.

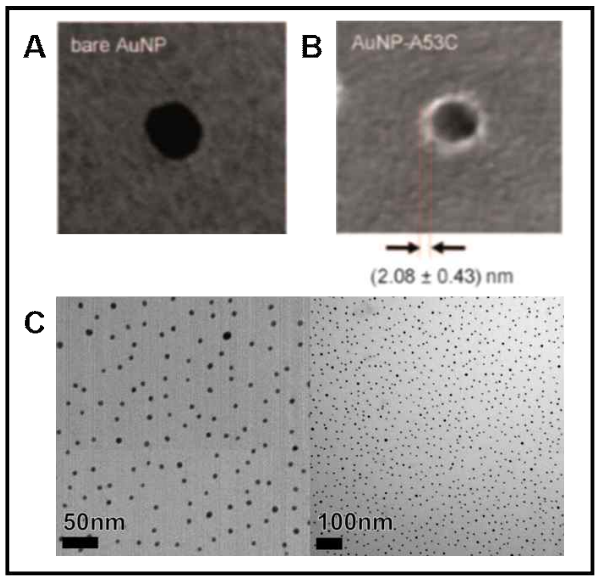

Figure 1. α-Synuclein coated AuNP (α-AuNP) TEM images of gold nanoparticles (A) Bare gold nanoparticle (B) α-synuclein protein coated gold nanoparticle, the protein layer surrounding the gold nanoparticle is visible after negative stain with 2% uranyl acetate. (C) α-AuNPs show high dispersity

Figure A and B: *Lee, D. et al. Angew. Chem. Int. Ed. 2011, 50, 1332-1337.

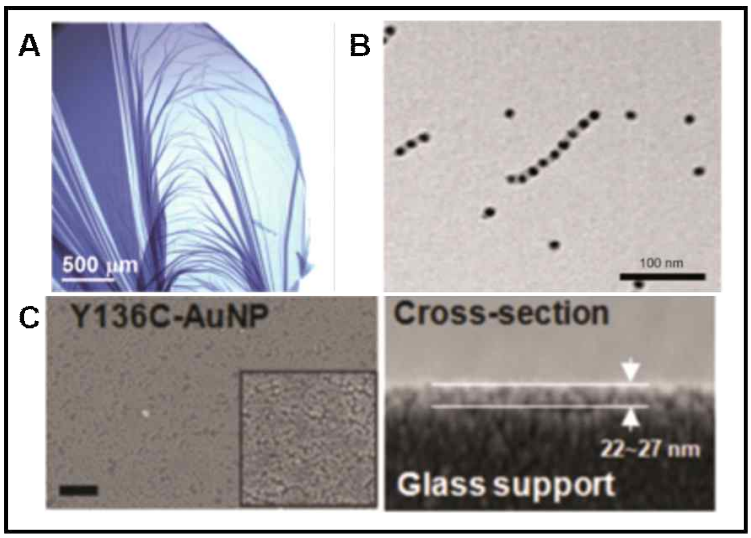

Figure 2. Infrastructure assemblies of α-AuNP (A) Optical image of α-AuNP free-standing film (B) TEM image of Pea-pod nano-chain assembly (C) Tight packing of α-AuNP on glass surface

Figure A: Lee, J. and Bhak G. et al. Angew. Chem. Int. Ed. 2015, 54, 4571-4576
Figure B: Lee, D. et al. Angew. Chem. Int. Ed. 2011, 50, 1332-1337
Figure C: Lee, D. et al. Langmuir 2011, 27, 12782-12787

1.3 Cancer Therapy by Drug Delivery System

1.3.1 Cancer Metastasis

Cancer is one of the deadliest disease to mankind causing enormous deaths globally every year. Significant development in the area of cancer therapy has been made for the past with improvement in diagnosis, surgical operation, and chemotherapy. [32] The conventional chemotherapy still has problems such as nonspecific distribution of drugs, excessive toxicity, and low targeting ability. [33] In order to overcome those obstacles, utilizing drug delivery system for cancer treatment has gathered interest of many scientists. [34] Therefore, an efficient drug delivery carrier with active targeting strategies would enhance the therapeutic efficacy in cancer treatment with minimizing toxic effect in normal cells. [33]

There are three major characteristics of cancer which are uncontrolled growth, mass formation and metastasis. [32] However, metastasis is considered to be the most fearsome and troublesome feature causing complexity to cancer therapy. [33,35] It is a process which tumor cells invade to surrounding tissues or into blood stream consequently forming metastases at other tissues. In cancer therapy, interfering cellular processes is an effective strategy thus inhibition of metastasis is thought to be a crucial target in cancer therapy. [36] Matrix metalloproteinase is known to be the potential target for therapeutics as the overexpession of this protien is associated with tumor invasion and metastasis. [36,37]

1.3.2 Matrix Metalloproteinase (MMP)

The matrix metalloproteinase are endopeptidase that belong to

the family of zinc-dependent proteinase. [36,37,38] They are involved in the degradation and remodelling of the extracelluar matrix. [36] More specifically, they consumes collagens as substrates and digest them. Subsequently, the digestion of extracelluar matrix facilitates tumor cells to be mobile and allow them to invade into blood vessels or lymph vessels. [37]

There are 18 members in the human MMP gene family which are structurely related and they are further categorized into five classes based on their structure and substrate specificity. [36] The five classes are collagenases, gelatinases, stromelysins, membrane type MMPs, and nonclassified MMPs. [36] Among them, type IV basement collagen digesting MMPs, MMP-2 and MMP-9, are the ideal drug targets because they are most consistently detected in tumor cells. [40]

Previous reports have indicated that there is a relationship between tumor metastasis and MMP overexpression. [40] Therefore, cancer researchers are actively designing and finding effective MMP inhibitors and developing drug delivery system that can successfully deliver MMP inhibitor to the cancer microenvironment. [36] When using DDS, a carrier must have a specific release mechanism that is responsive to selected stimuli. We believe the PoP system is expected to be responsive to the presence of MMPs as previous reports have proved reported that α-synuclein can be cleaved by MMPs. [37]

II. Materials and Methods

2.1 Materials

For the synthesis of mesoporous silica nanoparticles, tetraethylorthosilicate (TEOS) and hexadecyltrimethylammonium bromide (CTAB) were purchased from ACROS and sodium hydroxide (NaOH) and ethyl acetate (EtOAc) were purchased from Sigma Aldrich. Gold nanoparticles in 5nm size were purchased from Sigma Aldrich. 200-mesh carbon coated copper grids were purchased from Ted Pella Inc.. For the release profile, slide-A-Lyzer mini dialysis kit with 10,000 MWCO was purchased from ThermoFisher Scientific. Protease K was purchased from GenDEPOT and trypsin and chymotrypsin were purchased from Sigma Aldrich. Matrix Metalloproteinase-9 was purchased from AnaSpec. Nanopure water (18.1 MHz) was prepared from Direct-Q water purification system of Millipore. Other reagents used for protein purification were purchased from Sigma Aldrich.

2.2 Mesoporous Silica Nanoparticle Synthesis

50 mL of hexadecyltrimethylammonium bromide (CTAB) solution (0.1 g in 50 mL of nanopure water) was prepared and base (350 ul of 2M NaOH) was added. The mixture solution was heated to 75^{o}C and while gently stirring it 5 mL of tetraethylorthosilicate (TEOS) was added in dropwise manner. After 10 min, 0.5 mL of ethyl acetate (EtOAc) was added and the resulting mixture was vigorously stirred for 1 min and the sample was aged for 2.5 hour at the same temperature. After the aging, the solution turned to milky white and by

centrifugation white precipitate, MSN, was collected. The precipitate was resuspended in water and dispersed by water bath sonication. This washing step was performed twice with water and twice with ethanol. At last, to remove the CTAB from the pores of the synthesized MSN, 1.50 mL HCl was added to 150mL of MSN suspended ethanol solution then it was refluxed overnight.

2.3 Purification of α-Synuclein

Y136C α-synuclein DNA sequence was inserted into pRK172 plasmid. The resulting recombinant DNA was transformed in BL21 comeptent E.coli cell by heat-shock method. The cells were cultured on for 12 hours a LB agar plate containing 0.1 mg/ml ampicillin at 37^{o}C for screening. Then a colony is transferred into 100ml of LB media containing 0.1mg/ml ampicillin and incubated at 37^{o}C for 8 hours with shaking of 200rpm. After 8 hours, 1ml of the cultured solution was transferred into 1L of LB medium for the mass culture. The new media was incubated at same condition until the optical density at the wavelength of 600nm falls in the range between 0.6-0.8 then isopropano-b-D-thiogalactopyranoside (IPTG) was added for the induction of protein expression. Four hours later, the cells were harvested by centrifugation at 3600 rpm (Kontron) and the pellet was collected. The pellet was frozen and thawed first and resuspended in 200ml of lysis buffer containing (20mM tris/cl buffer, pH 7.5, 0.1M NaCl, 0.1mM PMSF, 1ug/ml Leupeptin, 2mM EDTA, 0.1mg/ml lysozyme and 10 units/ml of DNase). The cell lysate was centrifgued and surpernatant was collected and filtered through 0.22 um syringe filter. The protein crude extract was further purified by DEAE

Sephacyl anion exchange chromatography, S-200 Sephacryl Size exclusion chromatography and finally by S-sepharose cation exchange chromatograph. At each step, OD at 280nm was measured and noticeable peaks are verified by SDS-PAGE. After all three chromatograph steps, the protein solution was dialysed with 20mM MES buffer, pH 6.5, at 4^{o}C. The final protein solution was stored at −80^{o}C.

2.4 Preparation of the Protein Coated Gold Nanoparticles

50ul of 1mg/ml purified Y136C α-synuclein was mixed with 200ul of stock gold nanoparticle solution of 5nm. The resulting solution was incubated in a 4^{o}C refrigerator overnight. After incubation, the sample was centrifuged at 13200 rpm for 30minutes and discarded the supernatant. The pellet was washed with 200ul of MES buffer, pH 6.5, and the washing step was repeated twice more. The final pellet was collected and store in 4^{o}C.

2.5 Formation of Particles on a Particle (PoP)

Firstly, MSN was soaked in rhodamine6g dye solution to load the sample into the pores overnight. In a 1.5ml of transparent conical tube, 100ug of the MSN was reacted with 20 pmole of α-AuNP and the rest of the volume is filled with citrate buffer, pH 4.4, with the final volume of 100ul. The reaction has taken place for 2 hours then the PoP was collected by centrifugation at 9000rpm for 10min. The collected PoP was washed with 200ul of PBS buffer, pH 7.5, for 3 more times.

2.6 Characterization of MSN

The morphology and size of the synthesized MSN were observed on a transmission electron microscope(TEM) (JEM1010, JEOL, Jaoan) at 80 kV mode by loading sample on a carbon-coated copper grid. The particle size distribution was determined by a dynamic lgiht scattering (DLS) detector (Zetasizer Nano ZS, Malvern Co., UK). Using X-ray diffractometry (D8 Advance with Davinci, Bruker, Germany), low angle scan has been pursued to determine nanostructure of MSN. Nitrogen adsorption-desorption isotherms studies were carried by ASAP 2020 physisorption analyzer (USA). Before measurement the freeze dried MSN was degassed at 90^{o}C for 10 h to remove any contamination and moisture on the surface. Brunauer Emmett-Teller (BET) method was used to calculate the surface areas and the pore size distribution and pore volume were calculated by the Barrett-Joyner-Halenda (BJH) method.

2.7 UV/Vis Spectroscopy and FL Spectroscopy

Every UV/Vis measurement was conducted by UV/Vis spectrophotometer, Ultraspec 2100 Pro Amersham biosciences, USA. Also, all the fluorescence intensity of samples were measured by a fluorescence spectrometer, LS55, PelkinElmer, USA.

2.8 Cargo Release Assay

Cargo release from PoP was measured by placing slide-A-lyzer dialysis kit in a well plate. 200ul of PoP sample was pipetted into the dialysis kit and the well was filled with 1.5ml of PBS buffer and the solution in the well was measured for fluorescence intensity.

2.9 Enzyme Activity Assay

Hemoglobin substrate solution with concentration of 2.0% (w/v) was prepared by dissolving 0.2g of hemoglobin to 4ml of water. Then 800ul of 1M NaOH solution and 3.6g of urea was added to denature the hemoglobin. 50ul of 0.1units/ml enzyme solution was added to 250ul of the substrate solution. After selected time has passed, 500ul of TCA solution was added to precipitate down the undigested the proteins. The soluble peptide in the solution was collected by centrifugation and 150ul of F&C reagents were added to the solution. After letting the reaction to take place for 30 minutes, the absorbance of the solution was measured at 750nm.

III. Results and Discussions

3.1 Characterization of The Synthesized MSN

As illustrated on figure 3, the synthesis process of MCM-41 type of MSN was completed by using CTAB as the soft template for generating hexagonal pore array followed by sol-gel chemistry of the silica source, TEOS. In order to synthesize MSNs with uniform size of 100 nm and regular spherical morphology, the hydrolysis and the condensation reaction rates of the sol-gel chemistry was modulated. (Figure 3) The hydrolysis rate depends on the presence of NaOH, the base catalyst, and the condensation rate depends on the aging time hence establishing the optimal synthesis of MSN require modulation of these factors.

When the hydrolysis was uncontrolled and aging was proceeded afterward irregular shape of MSNs were synthesized. (Figure 4) Therefore, in order to control the hydrolysis rate, we have introduced ethyl acetate to scavenge the NaOH catalyst in the solution to dwindle the rate before proceeding to the condensation reaction. Furthermore, the aging time influenced the size of MSN, prolonging the aging time resulted in larger MSN, oppositely, shortening it resulted in smaller MSN. (Figure 4)

From these results, we have established the most optimal synthesis condition for regular spherical MSN with the size of 100 nm. The optimal condition involves letting the hydrolysis to take place to 10 minutes ethyl acetate was added then the aging was completed for 2.5 hours.

Under transmission electron microspocy (TEM), uniform size and shape of the resulting MSN was observed. (Figure 5) Also, dynamic light scattering was performed to further verify the size distribution of the MSN and it showed a narrow peak at 100 nm. (Figure 5) MCM-41 type of MSN has the defining hexagonal pore array nanostructure and to verify this Powder X-ray Diffraction (XRD) was conducted. The XRD pattern was measured at low angle from 0 to 10 and there are threes peaks indicating the miller indices of 100, 110, 200 hkl, which are the characteristic peaks observed from the hexagonal pore array structure. (Figure 5)

In addition, Brunauer-Emmett-Tell (BET) nitrogen gas adsorption-desoprtion isotherm analysis of powder form of the MSN was conducted to calculate the surface area as well as the Barrett-Joyner Halenda (BJH) analysis to calculate the pore size and

the volume. (Figure 6) The BET surface area was found to be 433.7221 g/m^2 and the BJH analysis verified pore size of 2.5 nm and pore volume of 0.79774 cm^3/g. (Table 1) Therefore, gold nanoparitcles with 5 nm in size are thought to be appropriate to block the pores with 2.5 nm in size and they are used in the PoP fabrication.

3.2 Confirmation of the fabricated PoP

As described earlier the particles-on-a-particle (PoP) drug delivery systems are fabricated by reacting α-AuNP and MSN at the isoelectric point of the protein, pH 4.4. (Figure 7) After the fabrication, TEM images of the PoP samples were taken and they show the α-AuNP are tightly clustered around MSN thus blocking the pores. (Figure 7). Even after several washing steps by centrifugation the PoP was stable thus indicating the considerably strong binding of the caps on the MSN. In other words, the PoP would be stable enough to endure the traveling through blood stream where it would experience shear pressure and colliding to other bio-molecules.

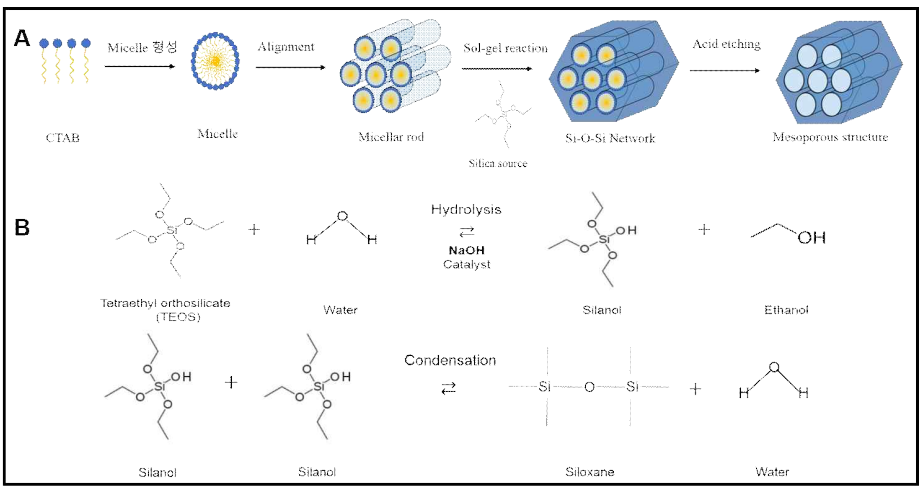

Figure 3. Synthesis of Mesoporous Silica Nanoparitcles (A) A Schematic illustration of MCM-41 type MSN synthesis process (B) Sol-gel Chemistry of tetraethylorthosilicate (TEOS)

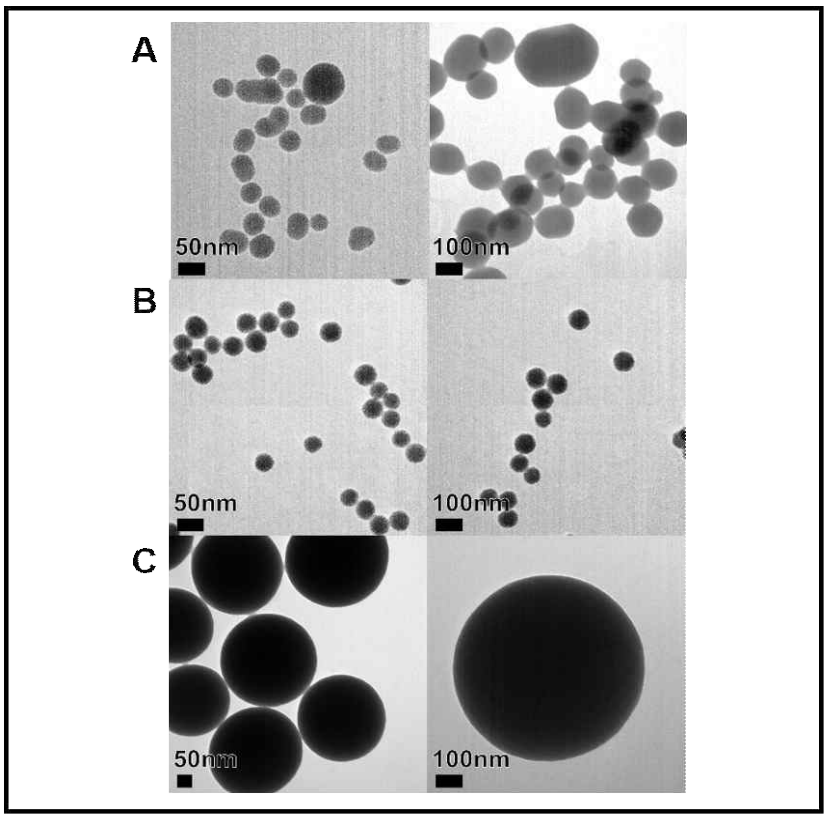

Figure 4. Size and morphology control of MSN TEM images of the synthesized MSN with different conditions (A) Without ethyl acetate treatment (B) Shortened aging time of 1 hour (C) Prolonged aging time of 4 hours.

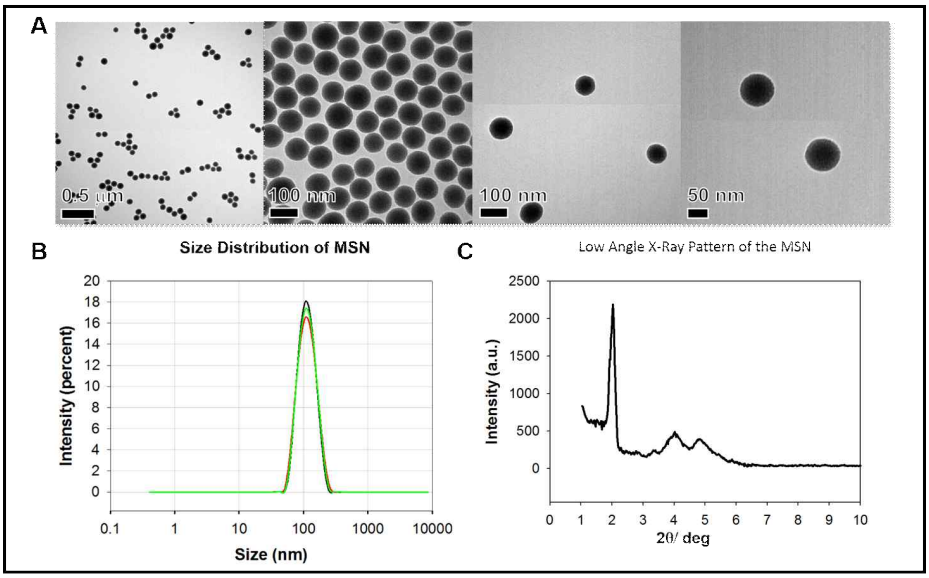

Figure 5. Analysis of the optimally synthesized MSN (A) TEM images of the spherical 100 nm MSN synthesized with the optimal condition (B) Dynamic Light Scattering (DLS) measurement showing narrow size distribution peak at 100 nm. (C) X-ray Diffraction (XRD) data showing three defining peaks of the hexagonal pore array at low angle.

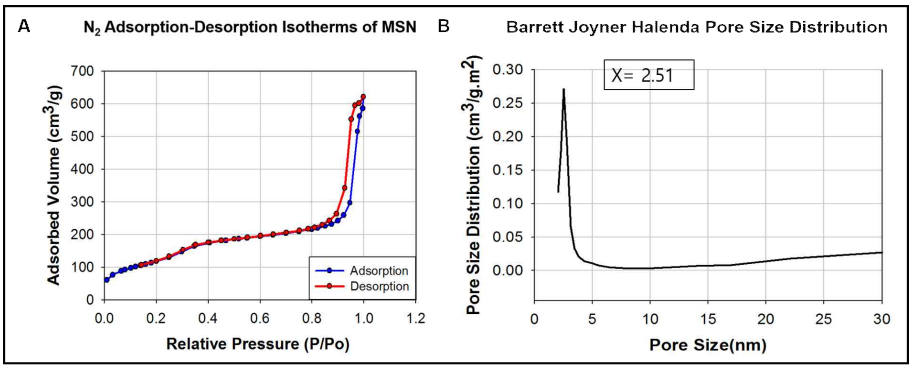

Figure 6. Brunauer-Emmett-Teller (BET) and Barrett-Joyner Halenda (BJH) Analysis (A) Nitrogen gas adsorption-desorption isotherm of the MSN (B) Graph of BJH pore size analysis

Diameter	BET Surface Area	Total Pore Volume	Pore Size	Zeta Potential
~100 nm	433.7221 (g/m^2)	0.79774 (cm^3/g)	2.5nm	-25.8

Table 1. Summary of the synthesized MSN characteristics

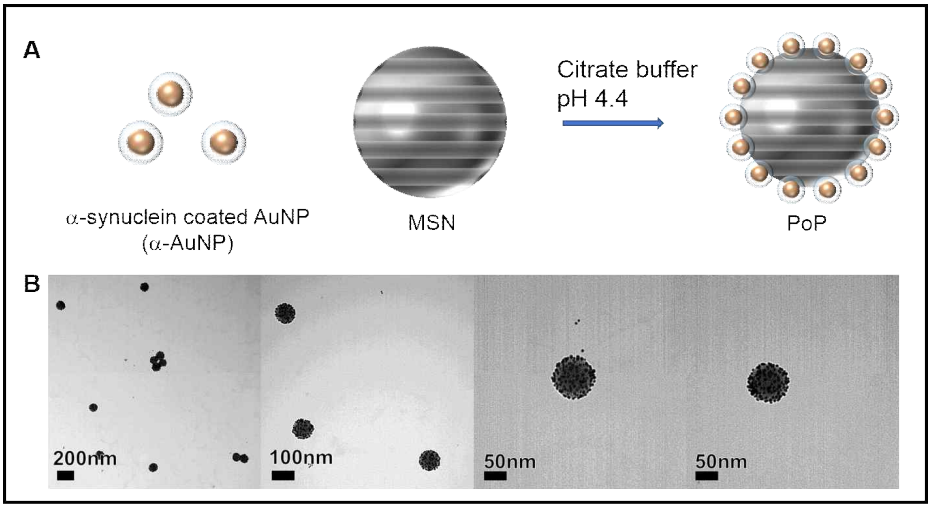

Figure 7. Fabrication of Particles-on-aParticle DDS (A) A Schematic illustration of PoP fabrication process (B) TEM images of PoP

3.3 Cargo Release Profile of Bare MSN vs. PoP

Cargo release profile was recorded using rhodamine6g (R6G) as the model cargo drug. The dye was loaded to MSN by suspending the MSN in R6G solution for overnight. Using a dialysis kit, the amount of R6G released to the solution was measured for bare MSN and PoP both loaded with the dye. Panel A in figure 8 is a graph which has been plotted by holding the florescence intensity measured for bare MSN sample at 300 minutes to be 100%. The graph shows a significant difference between the two samples, in comparison to bare MSN, PoP showed remarkably low cargo release. (Figure 8) More specifically, after 300 minutes, the R6G released from MSN was only 20% compared to that of MSN. Also, the TEM images of PoP after 300 minute demonstrate that the α-AuNPs were intactly blocking the pores. These results manifest the efficient gate keeping effect of PoP and its promising application as a drug carrier minimizing leaking of the loaded drug, in other words, preventing the side effects of the drug.

3.4 Effect of pH on The Cargo Release

Drug carriers travels through the physiological environment and experience various changes of the physico-chemical conditions, for example, the surrounding of tumor cells is acidic because they use glycolysis to botain extra energy. [34] For this reason, the effect of different pH on PoP was tested and likewise to the previous release profile cargo release was measured with R6G. In this test, PoP samples were placed in britton robinson buffers at different pH of 5, 6, 7, and 8. Within the measurement time of 300 minute, low cargo

release of around 20% was observed from all of the PoP samples at different pH. (Figure 9) Therefore, this indicates PoP drug delivery system is capable of enduring pH changes and maintaining efficient gate keeping.

3.5 Protease Induced Gate Opening of PoP

The cargo release results have manifested the effectiveness of the gate keeping capability of PoP. Since the α-AuNP caps are attached by the means of the adhesion characteristic of α-synuclein we expected presence of proteases would digest the protein consequently opening the gate. Therefore, the common proteases which are trypsin, protease K, and chymotrypsin were added to the R6G loaded PoP samples then the cargo release was measured.

It was observed that compared to the PoP without treatment, in all of the PoP samples treated with proteases, noticeably higher amount of R6G had been released during the time course of 30 minute. Also, the cargo release was highest in the PoP sample treated with trypsin and approximately 60 % was released after 300 minutes. This results also correlates to the abundance of lysin and arginine cleavage sites in the sequence of α-synuclein. TEM images of the samples treated with proteases after 300 minutes were taken to confirm the cap removal. (Figure 10) In all of the protease treated samples, the α-AuNPs were detached from MSN and found to be roaming in the solution.

These results indicate the gate opening of PoP can be achieved in the presence of PoP hence the system works in a controlled manner and it is enzyme responsive. Particularly, this suggests its potential application in protease activity control to protease sensors.

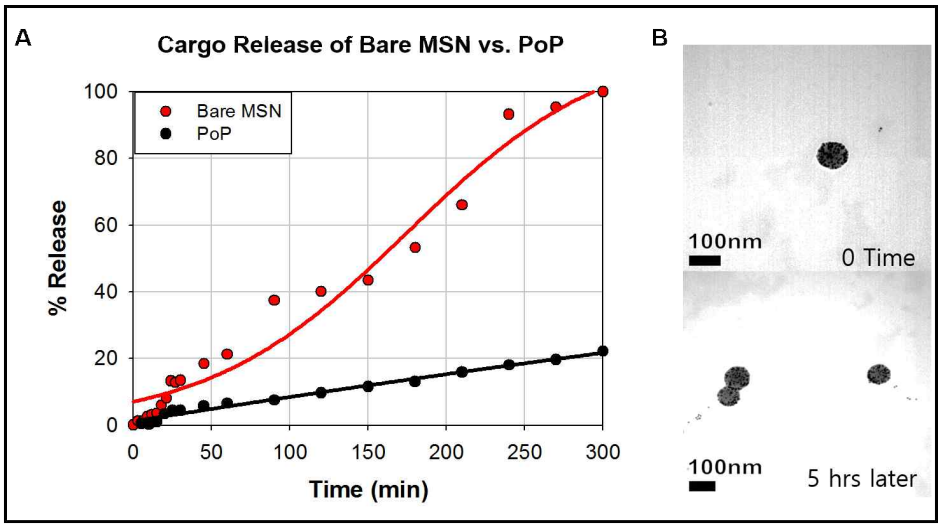

Figure 8. Cargo Release Profile of PoP vs. Bare MSN All samples were in PBS buffer of pH 7.5. Fluorescence intensity was measured to verify how much R6G has been released into the solution (A) Graph of the cargo releases of rhodamine6g (R6G) dye containing bare MSN and that of PoP. (B) TEM images of PoP at 0 time and 300 minutes later.

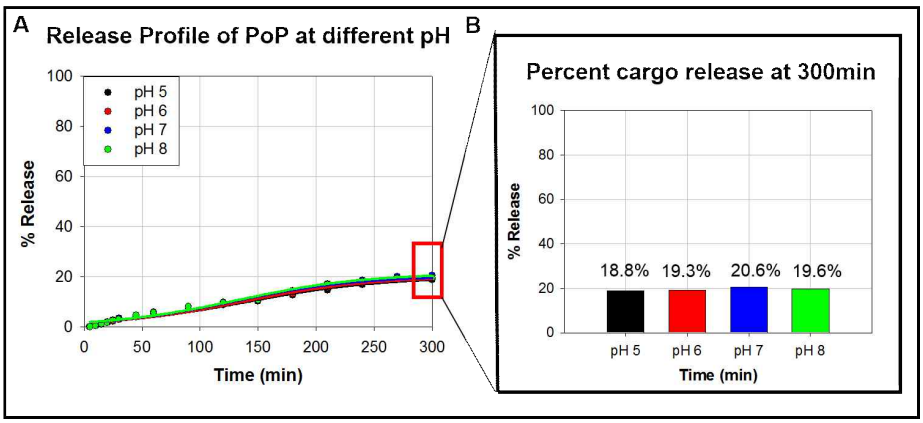

Figure 9. pH Effect on The Cargo Release of PoP R6G was used as the model cargo and Britton Robinson Buffer was used for pH control. (A) The Graph of percent cargo release of PoP samples at different pH for 300 minutes. (B) A bar graph of the amount released from each sample at 300 minute point.

3.6 Protease Activity Inhibition by PoP

The potential of PoP in the application of the inhibition of protease activity was verified with protease K using hemoglobin as substrate. In this test, the PoP samples were loaded with PMSF inhibitor and the digested substrate was quantified by measuring the amount of soluble peptide in the solution by reacting with Folin-Ciocalteu reagent.

The absorbance measurement graph shows highest digestion from the sample with protease only and lowest digestion from the samples with PMSF added as expected. (Figure 11) The PMSF loaded bare MSN also showed very low hemoglobin digestion and this is because the loaded PMSF are readily released since there is no gate control. The PMSF loaded PoP also manifested significant protease K inhibition effect, which means that the α-AuNP were detached from MSN by the digestion of protease K consequently the PMSF released from the pores successfully inhibited the protease K. Within the first 30 minutes, the digestion rate was higher for PoP compare to MSN due to the delay from the cap removal. After all, the results indicates the utiliity of PoP for inhibiting protease activity when loaded with inhibitors.

3.7 Matrix Metalloproteinase Induced Release

Finally, in order to show that PoP can be utilized for controlling the overexpression of MMP in the cancer metastasis process cargo release of PoP in the presence of MMP-9 was tested. Likewise to the previous assays R6G dye was used as model cargo and the fluorescence was measured for each sample treated with different MMP

concentrations. PoP without any proteases and PoP with trypsin treatment were set as the controls. In the presence of MMP, high fluoresence intensity compared to the control was observed and it seemed to correlate to the concentration of MMP treated. (Figure 12) Especially the sample with 30 ng/ul MMP-9 treatment showed noticeably high R6G release similar to the trypsin sample. Therefore, it is clear that the MMP-9 cleaved α-synuclein of the α-AuNP thus induced pore opening. Therefore, we can expect a promising application of PoP in MMP activity control, more specifically, a therapeutic strategy for cancer metastasis.

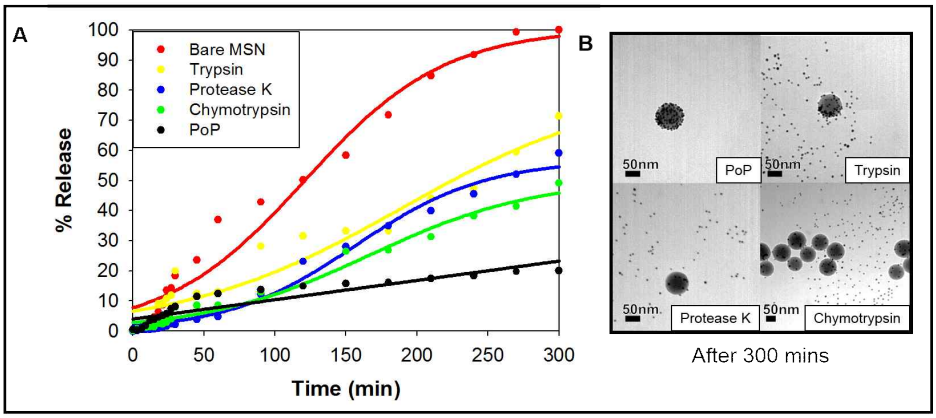

Figure 10. Proteases Induced Cargo Release of PoP The cargo release of PoP using R6G as the model drug was measured in the presence of different proteases. All protease concentrations were 30 ug/ul (A) A graph of R6G rhodamine release profile with samples incubated with the designated proteases. (B) TEM images of samples of PoP, trypsin treated PoP, protease K treated PoP, and chymotrypsin treated PoP after 300 minutes.

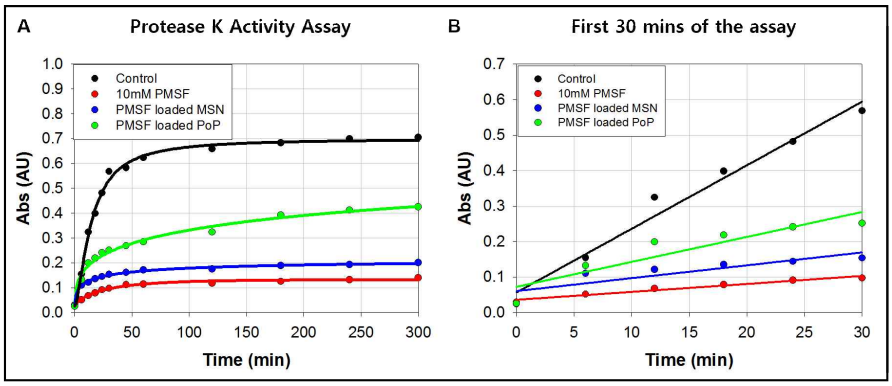

Figure 11. Protease K Activity Assay Urea denatured hemglobin was used as substrate for the assay. The soluble peptide digested by protease K was quantified by measuring the absorbance after reacting with Folin-Ciocalteu reagent (A) A graph showing change in protease K activity of samples of control (no treatment), 10mM PMSF, PMSF loaded MSN, and PMSF loaded PoP. (B) The first 30 minutes of the graph on the left.

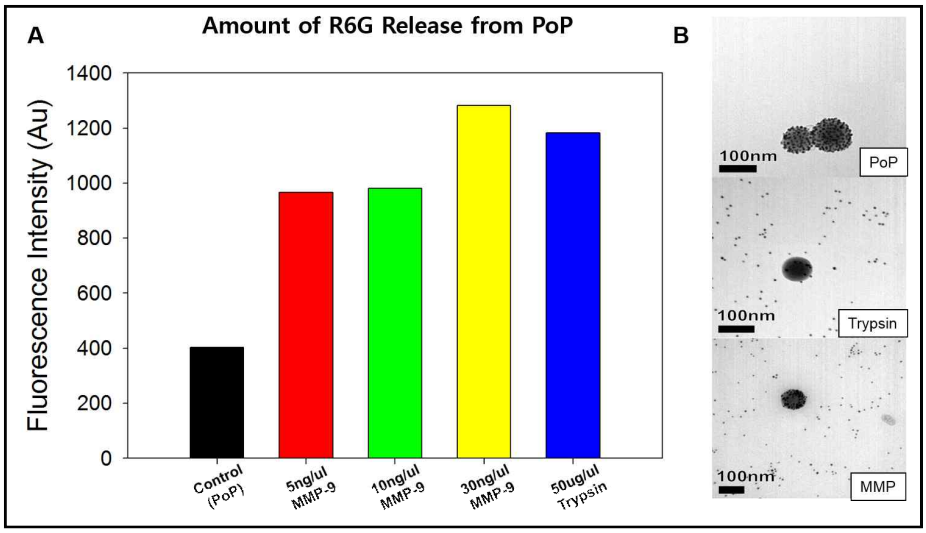

Figure 12. MMP Induced Cargo Release from PoP Rhodamine6G dye was used as the model cargo and the fluorescence of the supernatant was measured after incubation with the assigned protease type and concentration at 37 for 1 hour. (A) A bar graph of the fluorescence intensity measured for each sample. (B) TEM images of the PoP samples after incubation.

IV. Conclusions

In this research, we have introduced particles-on-a-particle carrier model which is a novel drug delivery system with remarkable gate keeping effect and controllable cargo release mechanism. We began with demonstrating the fabrication process of PoP including synthesis of mesoporous silica nanoparticle followed by assays for cargo release profile of PoP, cargo release from PoP by protease digestion, usage of PoP for inhibiting protease activity, and finally MMP responsive cargo release.

First of all, in the MSN synthesis part, we were able to synthesize uniform 100 nm MSNs with spherical shape by modulating the hydrolysis rate and the condensation rate of sol-gel chemistry of silica. The resulting MSNs were analyzed by TEM, DLS, XRD, and BET/BJH for determining the size distribution, morphology, surface area, nano-structure, and pore size and volume. Table 1 shows the summary of the characteristics of the synthesized MSN. After obtaining MSNs, they were incubated with α-AuNP in citrate buffer of pH 4.4 and the intact PoP fabricated and were verified by TEM analysis.

Next, the cargo release profile of R6G model cargo revealed the secured gate keeping effect as well as its stability at various pH ranges. In addition, PoP demonstrated that the controlled cargo release was achieved by the digestion of proteases meaning that PoP system could be utilized for applications like protease sensor for conditions where change in level of certain proteases is important. Then utilizing PoP for inhibiting protease K activity was carried out and PoP

effectively inhibited the protease indicating that same consequence can be expected for controlling MMP activity.

Finally, a successful cargo release of the R6G containing PoP was observed in the presence of MMP-9 indicaitng that PoP is MMP responsive. Therefore, it is likely that PoP DDS can be applied for the MMP activity control which is the crucial target in cancer metastasis process. This means that PoP has a promising potential as a drug delivery carrier for the treatment of diseases where controlling certain type of protease is the key factor.

V. References

[1]. JunSeok, Lee, Juhee Park, Kaushik Singha and Won Jong Kim (2012) Mesoporous silica nanoparticle facilitated drug release through cascade photosensitizer activation and cleavage of singlet oxygen sensitive linker. *ChemComm*, 49, 1545-1547.

[2]. Igor I., Slwoing, Brian G. Trewyn, Supratim Giri, and Victor S.Y. Lin (2007) Mesoporous Silica Nanoparticles for Drug Delivery and Biosensing Applications. *Adv. Funct. Mater.*, 2007, 17, 1225-1236.

[3]. Zongxi Li, Jonathan C. Barnes, Aleksandr Bosoy, J. Fraser Stoddart and Jeffrey I. Zink (2012) Mesoporous silica nanoparticles in biomedical applications. *Chem. Soc. Rev*., 2012, 41, 2590-2605

[4]. Xin Chen, Xiaoyu Cheng, Alexander H. Soeriyadi, Sharon M. Sagnella, Xun Lu, Jason A. Scott, Stuart B. Lowe, Maria Kavallaris, and J. Justin Gooding (2014) Stimuli-responsive functionalized mesoporous silica nanoparticles for drug release in response to various biological stimuli. *Biomater. Sci*., 2, 121-130

[5] Fangqiong Tang, Linlin Li, and Dong Chen (2012) Mesoporous Silica Nanoparticles: Synthesis, Biocompatibility and Drug Delivery. *Adv. Mater,* 2012, 24, 1504-1534

[6] Qianjun He and Jianlin Shi (2011) Mesoporous silica nanoparticle based nano drug delivery systems: synthesis, controlled drug release and delivery, pharmacokinetics and biocompatibility. *J. Mater. Chem.*, 2011, 21, 5845-5855

[7] Kevin C.-W. Wu and Yusuke Yamauchi (2012) Controlling physical features of mesoporous silica nanoparticles (MSNs) for emerging applications. *J. Mater. Chem.*, 2012, 22, 1251-1256

[8] Supratim Giri, Brian G. Trewyn, Michael P. Stellmaker, and Victor S.-Y. Lin (2005) Stimuli-Responsive Controlled-Release Delivery System Based on Mesoporous Silica Nanorods Capped with Magnetic Nanopaticles. *Angew. Chem. Int. Ed.* 2005, 44, 5038-5044

[9] Buckley, A.M. and Greenblatt, M.J. (1994) Sol-Gel Preparation of Silica Gels.

Chem. Ed. 1994, 71(7), 599

[10] Igor I. Slowing, Juan L. Vivero-Escoto, Chia-Wen Wu, and Victor S.-Y. Lin (2008) Mesoporous Silica Nanoparticle as controlled release drug delivery and gene transfection carriers. *Advanced Drug Delivery Reviews*, 2008, 60, 1278-1288

[11] Ji Eun Lee, Nohyun Lee, Hyoungsu Kim, Jaeyun Kim, Seung Hong Choi, Jeong Hyun Kim, Taeho Kim, In Chan Song, Seung Pyo Park, Woo Kyung Moon, and Taeghwan Hyeon (2010) Uniform Mesoporous Dye-Doped Silica Nanoparticles Decorated with Multiple Magnetite Nanocrystals for Simultaneous Enhanced Magnetic Resonance Imaging, Fluorescence Imaging, and Drug Delivery. *J. Am. Chem. Soc.* 2010, 132, 552-557

[12] Qianjun He and Jialin Shi (2014) MSN Anti-Cancer Nanomedicines: Chemotherapy Enhancement, Overcoming of Drug Resistance, and Metastasis Inhibition. *Adv. Mater.* 2014, 26, 391-411

[13] Igor Slowing, Brian G. Trewyn, and VIctor S.-Y. Lin (2006) Effect of Surface Functionalization of MCM-41 Type Mesoporous Silica Nanoparticles on the Endocytosis by Human Cancer Cells. *J. AM. Chem. Soc.* 2006, 128, 14792-14793

[14] Jessica M. Rosenholm, Cecilia Sahlgren and Mika Linden (2010) Towards multifunctional, targeted drug delivery systems using mesoporous silica nanoparticles − opportunities & challenges. *Nanoscale,* 2010, 2, 1870-1883

[15] Yanna Cui, Haiqing Dong, Xiaojun Cai, Deping Wang, and Yongyong Li (2012) Mesoporous Silica Nanoparticles Capped with Disulfide-Linked PEG Gatekeepers for Glutathione-Mediated Controlled Release. *Appl. Mater. Interfaces* 2012, 4, 3177-3183

[16] Amirali Popat, Sandy Budi Hartono, Frances Stahr, Jian Liu, Shi Zhang Qiao and Gao Qing (Max) Lu (2011) Mesoporous Silica Nanoaprticle for bioadsorption, enzyme immobilisation, and delivery carriers. *Nanoscale,* 2011, 3, 2801

[17] Juan L. Vivero-Escoto, Igor I. Slowing, Chian-Wen Wu, and Victor S.-Y. Lin (2009) Photoinduced intracellular Controlled Release Drug Delivery in Human Cells by Gold-Capped Mesoporous Silica Nanosphere. J. Am. Chem. Soc. 2009, 131, 3462-3463

[18] Piaoping Yang, Shili Gai, and Jun Lin (2012) Functionalized mesoporous silica materials for controlled drug delivery. *Chem. Soc. Rev.,* 2012, 41, 3679-3698

[19] Kristina Riehemann, Stefan W. Schneider, Thomas A. Luger, Biana Godin, Mauro Ferrari, and Harald Fuchs (2009) Nanomedicine-Challenge and Perspectives.

Angew. Chem. Int. Ed., 2009, 48, 872-897

[20] Cheng-Yu Lai, Brian G. Trewyn, Dusan M. Jeftinija, Ksenija Jeftinija, Shu Xu, Srdija Jeftinija, and Victor S.-Y. Lin (2003) A Mesoporous Silica Nanosphere-Based Carrier System with Chemically Removable CdS Nanoparticle Caps for Stimuli-Responsive Controlled Release of Neurotransmitters and Drug Molecules. *J. Am. Chem. Soc.*, 2003, 125, 4451-4459.

[21] Maria Grazia Spillantini, Marie Luise Schmidt, Virginia M.-Y. Lee, John Q. Trojanowski,, Ross Jakes, and Michel Goedert (1997) α-synuclein in Lewy Bodies., Nature, 1997, vol 388, 28

[22] Minami Baba, Shiegeo Nakajo, Pang-Hsien Tu, Taisuke Tomita, Kazuyasu Nakaya, Virginia M.-Y. Lee, John Q. Trojanowski, and Takeshi Iwatsubo (1998) Aggregation of α-synuclein in Lewy Bodies of Sporadic Parkinson's Disease and Dementia with Lewy Bodies, *American Journal of Pathology,* Vol 152, No 4, April 1998

[23] C. B. Lucking and A. Brice (2000) Alpha-synuclein and Parkinson's disease. CMLS, *Cell. Mol. Life Sci.* 57 (2000) 1894-1908

[24] P.M. Mattila, J. O. Rinne, H. Helenius, D. W. Dickson, and M. Roytta (2000) Alpha-synuclein-immunoreactive cortical Lewy bodies are associated with cognitive impairment in Parkinson's disease. *Acta Neuropathol* (2000) 100: 285-290

[25] Benoit I. Giasson, Mark S. Forman, Makoto Higuchi, Lawrence I. Golbe, Charles L. Graves, Paul T. Kotzbauer, John Q. Trojanowski, Virginia M.-Y. Lee (2003) Initiation and Synergistic Fibrillization of Tau and Alpha-Synuclein. *Science* 300, 636 (2003)

[26] Tiago Fleming Outeiro and Susan Lindquist (2003) Yeast Cells Provide Insight into Alpha-Synuclein Biology and Pathobiology., *Science* 302, 1772 (2003)

[27] Pavan K. Auluck, Gabriela Caraveo, and Susan Lindquist (2010), α-synuclein: Membrane Interactions and Toxicity in Parkinson's Disease., Annu. Rev. Cell Dev. Biol. 2010. 26:211-33

[28] Daekyun Lee, Young-Jun Choe, Minwoo Lee, Dae H. Jeong, and Seung R. Paik (2011) Protein-Baesd SERS Technology Monitoring the Chemical Reactivity on an α-synuclein-medicated Two-Dimensional Array of Gold Nanoparticles., Langmuir 2011, 27, 12782-12787

[29] Daekyun Lee, Je Won Hong, Chanyoung Park, Hagyeol Lee, Ji Eun Lee,

Taeghwan Hyeon, and Seung R. Paik (2014) $Ca2^{+}$-Dependent Intracellular Drug Delivery System Developed with "Raspberry-Type" Particles-on-a-Particle Comprising Mesoporous Silica Core and α-Synuclein-Coated Gold Nanoparticles., *Acs Nano,* 2014, Vol 8, No. 9, 8887-8895

[30] Daekyun Lee, Young-Jun Choe, Yeon Sun Choi, Ghibom Bhak, Jihwa Lee, and Seung R. Paik (2011) Photoconductive of Pea-Pod-Type Chains of Gold Nanoparticles Encapsulated within Dielectric Amyloid Protein Nanofibrils of α-Synuclein. *Angew. Chem. Int. Ed.,* 2011, 50, 1132-1337

[31] Junghee Lee, Ghibom Bhak, Ji-Hye Lee, Woohyun Park, Minwoo Lee, Daekyun Lee, Noo Li Jeon, Dae H. Jeong, Kookheon Char, and Seung R. Paik (2015) Free Standing Gold-Nanoparticle Monolayer Film Fabricated by Protein Self-Asembly of α-Synuclein., *Angew. Chem. Int. Ed.,* 2015, 54, 4571-4576.

[32] Isaiah J. Fidler (2003) The pathogenesis of cancer metastasis: the 'seed and soil' hypothesis revisited, *Nature Reviews*, volume 3, 1-6

[33] Wadih Arap, Renata Pasqualini, and Erkki Ruoslahti (1998) Cancer Treatment by Targeted Drug Delivery to Tumor Vasculature in a Mouse Model, *Science*, 279, 377

[34] Kwangjae Cho, Xu Wang, Shuming Nie, Zhuo (Georgia) Chen, and Dong M. Shin (2008) Therapeutic Nanoparticles for Drug Delivery in Cancer, *Clin. Cancer Res*., 2008; 14:1310-1316

[35] John F. R. Kerr, Clay M. Winterford, Assoc. Dipl. Appl. Biol., and Brian V. Haromon (1994) Apoptosis, *Cancer*, 1994, Volume 73, No. 8

[36] Manuel Hidalgo, S. Gail Eckhardt (2001) Development of Matrix Metalloproteinase Inhibitors in Cancer Therapy, *Journal of the National Cancer Institute*, Vol.93, No. 3

[37] Johannes Levin, Armin Giese, Kai Boetzel, Lars Israel, Tobias Hogen, Georg Nubling, Hans Kretzschmar, and Stefan Lorenzl (2008) Increased α-synuclein aggregation following limited cleavage by certain matrix metalloproteinases, *Experimental Neurology*, 215, 201-208

[38] M.W. Roomi, J.C. Monterrey, T. Kalinovsky, M. Rath and A. Niedzwiecki (2009) Patterns of MMP-2 and MMP-9 expression in human cancer cell lines, *Oncology Reports,* 21: 1323-1333

[39] Gabriele Bergers, Rolf Brekken, Gerald McMahon, Thiennu H. Vu, Takeshi Itoh, Kazuhiko Tamaki, Kazuhiko Tanzawa, Philip Thorpe, Shigeyoshi Itohara, Zena Werb,

and Douglas Hanahan (2000) Matrix Metalloproteinase-9 triggers the angiogenic switch during carcinogenesis, *Nature Cell Biology,* Vol 2

[40] Stanley Zucker and Jian Cao (2009) Selective Matrix metalloproteinase (MMP) inhibitors in cancer therapy: ready for prime time?, *Cancer Biol Ther.* 2009; 8(24): 2371-2373

국문 초록

최근 몇 년 동안 라이포좀, 나노캡슐, 합성 폴리머 등과 같은 다양한 약물전달 시스템들이 약물의 치료효과를 극대화하기 위한 목적으로 지속적으로 개발되어 왔다. 그러나 선택적 약물 방출이 가능한 새로운 게이트 방지 시스템 기작을 개발하는 것은 아직까지 풀어야할 숙제이다. 본 연구에서는 프로테아제의 반응하며 효과적인 게이트 방지 능력를 지닌 약물전달 시스템의 제작과 암 전이 조절을 위한 응용으로서의 가능성을 제시한다.

본 약물전달 시스템은 다공성의 실리카 나노입자를 기반으로 하며 α-synuclein 단백질의 특이적인 흡착 성질을 이용하여 이 단백질로 코팅되어진 금나노입자로 다공을 막는다. 우리는 많은 금나노입자들이 하나의 실리카 나노입자를 감싸고 있는 모양을 바탕으로 이 약물전달 시스템을 Particles-on-a-Particle (PoP)으로 명명하였다.

Rhodamine6G 형광물질을 이용한 in vitro 약물방출 연구를 통해 PoP의 확실한 게이트 관리 효과를 증명하였으며 다양한 pH 조건에서도 안정함을 확인하였고 이는 곧 약물이 무작위로 방출되는 것을 방지할 수 있음을 의미한다. 더 나아가 선택적인 약물방출이 trypsin, protease K 그리고 chymotrypsin과 같은 프로테아제로 인해 가능한 것을 확인하였다. 또한 프로테아제의 억제제를 탑재한 PoP을 이용하여 프로테아제에 의한 억제제가 방출과 이로 인한 해당 프로테아제의 억제가 가능하다는 것을 확인하였다.

마지막으로 암전이 과정에서 extracelluar matrix를 분해시키는 중요한 타겟으로 여겨지는 Matrix metalloproteinase의 과발현 조절을 위한 활용을 목적으로 MMP에 의한 PoP에 약물방출을 확인하였다. 이를 통해 상당한 양의 탑재된 약물이 MMP에 의해 방출이 되는

것을 관찰하였으며 이러한 결과들은 효소 반응적인 치료용 나노캐리어로서의 PoP의 가능성을 강조한다. 그리고 이는 곧 약물의 조절되지 못한 소실의 방지를 의미한다. 마지막으로 PoP이 생체내에 병리적 물리화학적 변화에 반응하는 효과적인 약물전달체가 될 수 있을 것이라 기대된다.

주요 단어: **α-synuclein, Mesoporous Silica Nanoparticle, Drug Delivery System, Matrix Metalloproteinase, Protease Inhibition, Gate Control, Cancer Metastasis.**

학번: 2013-23163